NATIONAL ADVISORY COMMITTEE FOR AERONAUTICS

WARTIME REPORT

ORIGINALLY ISSUED
August 1945 as
Advance Restricted Report L5F30a

HINGE MOMENTS OF SEALED-INTERNAL-BALANCE ARRANGEMENTS FOR CONTROL SURFACES

II - EXPERIMENTAL INVESTIGATION OF FABRIC SEALS IN THE PRESENCE OF A THIN-PLATE OVERHANG

By Jack Fischel

Langley Memorial Aeronautical Laboratory
Langley Field, Va.

NACA

WASHINGTON

NACA ARR No. L5F30a

NATIONAL ADVISORY COMMITTEE FOR AERONAUTICS

ADVANCE RESTRICTED REPORT

HINGE MOMENTS OF SEALED-INTERNAL-BALANCE ARRANGEMENTS FOR CONTROL SURFACES

II - EXPERIMENTAL INVESTIGATION OF FABRIC SEALS IN THE PRESENCE OF A THIN-PLATE OVERHANG

By Jack Fischel

SUMMARY

Tests were made in a seal test chamber to determine the hinge moments contributed by the fabric seal in an internal-balance arrangement employing a thin-plate overhang. These tests were performed with various widths of fabric sealing various widths of flap-nose gap, with a horizontal, a vertical, and a circular type of wing structure forward of the balance, and with various heights of balance chamber.

This investigation is an experimental verification and extension of a previous analytical investigation. The present investigation indicated that the moment of the seal may be a balancing or an unbalancing moment and may be an appreciable part of the total balancing moment of an internally balanced flap, depending on the overhang deflection and the configuration of the internal balance. Variation of the width of the fabric seal, the sealed gap, or the location of the seal attachment to the wing structure affected the seal moments through most of the overhang deflection range. The shape and size of the balance chamber affected the seal-moment characteristics in the deflection range where the seals contacted and were constrained by the chamber walls; the values of the seal moments were usually reduced when the seals were constrained. The results indicated also that an optimum balance configuration would employ a seal width such that the seal would barely touch the chamber ceiling when maximum overhang deflection is attained.

INTRODUCTION

One of the devices employed for balancing control surfaces, especially ailerons, of modern high-speed airplanes is the sealed internal balance (fig. 1). Much of the experimental work that has been done in the development of the sealed internal balance has been summarized in reference 1, which includes a brief consideration of seal effects. In reference 1 (and in all previous internal-balance work), the balancing effect of a seal in an internal-balance arrangement was accounted for by an approximate method - that is, by assuming the balance chord to be the distance from the control-surface hinge axis to the center of the sealed nose gap, regardless of seal width.

An analytical investigation to determine the contribution of the seal to the balancing moment of a sealed-internal-balance arrangement indicated that the approximate method was generally in error over most of the flap-deflection range (reference 2). This analysis also indicated that variation of either the seal width, the sealed-gap width, or the shape of the wing structure forward of the overhang has an important effect on the balancing moment contributed by the seal.

The present investigation is an extension of the investigation reported in reference 2 and was begun in order to check experimentally the fabric-seal analysis reported therein. The present investigation covered a larger deflection range than was covered in reference 2; in addition, the effect on the seal moments of a confining balance-chamber roof (the contour of the airfoil) and an off-center attachment of the seal to the wing structure were determined.

The moment contributed by the seal in each of the configurations tested is presented as a fraction of the moment of the thin-plate overhang over the complete deflection range. A comparison is made of the seal moments obtained experimentally and analytically (reference 2) with seals and sealed nose gaps of similar size in the presence of each of the three different types of internal wing structure with no vertical restrictions. In addition, a comparison is made between the experimentally determined and the computed hinge-moment coefficients of an internally balanced aileron, and an

example is presented to show the relative accuracy of hinge-moment data computed by the approximate method and those computed from the results of the present investigation.

SYMBOLS

m_s seal-moment ratio (M_s/M_b)

c_{h_a} aileron section hinge-moment coefficient $\left(h_a/qc_a^2\right)$

Δc_{h_a} increment in aileron section hinge-moment coefficient produced by an internal-balance arrangement

P_R pressure coefficient across balance (pressure below balance minus pressure above balance divided by dynamic pressure)

δ_b thin-plate overhang deflection, degrees; positive when deflection is increased from neutral by pressure across balance

δ_{b_l} limiting deflection of thin-plate overhang, degrees (deflection just prior to contact between leading edge of overhang and roof of test chamber (contour of airfoil))

δ_a aileron deflection with respect to airfoil chord line, degrees

M_b moment of thin-plate overhang (used with subscripts exp and comp to indicate experimental and computed, respectively), foot-pounds

M_s moment of seal, foot-pounds

g width of sealed gap between points of attachment of seal when $\delta_b = 0^\circ$, fraction of c_b

s seal width, fraction of c_b

h_a aileron section hinge moment, foot-pounds

t thickness of overhang at hinge axis, fraction of c

c	airfoil chord, feet except when otherwise indicated
c_a	aileron chord behind the hinge line, fraction of c
c_b	overhang chord from flap hinge line to leading edge of overhang, fraction of c
q	dynamic pressure, pounds per square foot $\left(\frac{1}{2}\rho V^2\right)$
V	absolute velocity of air stream, feet per second
ρ	mass density of air, slugs per cubic foot
M	Mach number (V/a)
a	velocity of sound in air stream, feet per second
α	angle of attack, degrees

APPARATUS AND METHODS

The seals were tested in a specially prepared seal test chamber that simulated the construction of an internal-balance chamber ahead of the flap hinge line (figs. 2(a) and 2(b)). The span of the overhang was 24 inches and the chord was 10 inches from the hinge line to the leading edge. The thin-plate overhang was rigidly attached to a torque tube that was, in turn, attached to a dial outside the test chamber and deflected the overhang through the test range. A clearance of 3/64 inch was allowed at each end of the overhang span to prevent contact with the side walls through the deflection range. A small clearance behind the hinge line between the torque tube and the test-chamber structure was sealed with a small fabric seal; the moment produced by the seal was considered in the calculations. The difference in normal pressure existing across the seal and overhang of an internal-balance arrangement was simulated by the controlled pressure produced in the part of the test chamber below the overhang by a blower, while atmospheric pressure existed above the overhang. The pressure across the overhang and seal was indicated by a micromanometer and this pressure was maintained at approximately 17 pounds per square foot by a door on the blower intake. The distribution of pressure in the region below the overhang

and the seal was determined from a brief survey to be uniform within approximately ±1 percent; a pressure drop of approximately 15 to 20 percent was found to occur within 1/16 inch of either end of the overhang span, about which a flow took place, but the effect of this pressure difference on the hinge moments is believed to be negligible.

One of the chordwise chamber walls was made of plexiglass through which photographs were taken of the seal profile under various conditions.

The hinge moments of the balance arrangement were determined by means of a calibrated torque-rod system built for this setup (figs. 2(a) and 2(b)). The overhang deflection was determined by the reading of the overhang-deflection dial with respect to a pointer attached to the outer wall of the test chamber (fig. 2(a)).

Three types of balance-chamber structure ahead of the overhang were used in the investigation. These surfaces are shown in figure 2(a) and are referred to herein as backplates. The backplates were of uniform height and span; their chordwise positions were varied during the tests to give various sizes of gap. The seals tested were made of Koroseal, which is an airtight, flexible, fabric material, and had a varying chord width and a span equal to that of the overhang. A thin metal strip was fastened along the span at both ends of each seal to attach the seal to the backplate and to the leading edge of the overhang (fig. 2(a)).

The vertical balance-chamber restriction (contour of the airfoil) was simulated by a horizontally held plate; the distance of this plate above the overhang and seal was varied to give the proper value of δ_{b_l}. For uniformity and agreement with reference 2, all the linear dimensions of the balance configuration are expressed as a fraction of the overhang chord.

A list of the balance configurations tested is given in table I. Since the pressure difference across the balance of a control surface does not always reverse when the control is neutral, tests were made at negative deflections up to -12° and the tests were run with the overhang deflection varying in 2° and 4° increments up to 30° or the maximum deflection allowed by the seal or

overhang. The results are applicable to both negative and positive flap-deflection ranges, however, and the change in direction of the balancing moment is determined by the deflection at which the sign of the pressure difference across the balance changes.

In obtaining the hinge moment due to the seal, the moment of the overhang had to be subtracted from the total moment of overhang and seal measured by the torque system. The moment of the overhang alone, without any seal present, was obtained over the deflection range by closing the gap between the overhang nose and the backplate to a very small value. Because of the large leakage area for this condition, a pressure difference of only about 10 pounds per square foot, considerably less than the normal test pressure, could be maintained. The overhang moment thus obtained experimentally was compared with the overhang moment computed from the thin-plate dimensions and the pressure difference across the overhang. The experimental moment was found to be approximately 1 percent higher than the computed moment. The seal moments were therefore obtained by subtracting the computed overhang moment, corrected for the 1-percent discrepancy, from the total moment measured in each test.

The computations for obtaining the seal-moment ratio are indicated in the following equation:

$$m_s = \frac{M_s}{M_b} = \frac{M_{\text{total exp}} - 1.01\, M_{b_{\text{comp}}}}{1.01\, M_{b_{\text{comp}}}}$$

RESULTS AND DISCUSSION

Seal-Profile Photographs

Some typical profiles and positions of the seals with a pressure difference across the balance are shown in figures 3 to 7 with a vertical backplate, in figures 8 and 9 with a circular backplate, and in figures 10 to 13 with a horizontal backplate. The constraining effect on the profile of the seal caused by the vertical and circular backplates in the positive deflection range is shown in figures 3, 4, and 9; whereas figure 10 indicates

that the horizontal backplate had little or no confining effect. Similarly, figures 5, 7, 8, 11, and 12 indicate the confining effect of an overhead restriction simulating the top or bottom of the balance chamber. When a seal was free to billow unrestricted by backplate or overhead limit, the seal generally tended to assume a circular shape. This fact, which formed the basis for the analytical work of reference 2, is illustrated in figure 10(d) by a circle superimposed on an enlargement of the photograph of figure 10(b).

Desired Seal-Moment Characteristics

A desired variation of the seal-moment ratio m_s with overhang deflection is one that offers a positive value of the slope $\partial m_s/\partial \delta_b$ with deflection. (See reference 2.) This variation of m_s with deflection would tend to compensate for the decrease in the variation of pressure coefficient across the balance P_R with deflection (that is, the decrease in $\partial P_R/\partial \delta_b$) as the deflection increases and to provide more nearly linear balance hinge moments and control forces.

Experimental Seal-Moment Characteristics

The seal-moment characteristics over the deflection range for various sizes of fabric seal and sealed nose gap, without and with overhead limits, are shown in figures 14 to 21 when the seals were tested with a vertical backplate, in figures 22 to 26 with a circular backplate, and in figures 27 to 34 with a horizontal backplate.

With all three types of backplate, the moment exerted by the seal in the balancing configuration is appreciable, particularly with large seals and large sealed gaps. This seal moment may be a balancing moment amounting to as much as 40 or 50 percent of the overhang balancing moment, or it may be an unbalancing moment amounting to as much as 30 or 40 percent of the overhang balancing moment, depending on the overhang deflection and the configuration of the internal balance. Negative values of m_s were sometimes obtained with all three types of backplate in the negative deflection range and over a small portion of the positive deflection range near zero

deflection (figs. 14, 15, 22, 27, and 28). In these configurations the seal overlapped a part of the overhang, which equalized the pressure on both sides of this part of the balance and tended to reduce the amount of effective balance available. A configuration illustrating this tendency was not photographed, but this condition is approached in figure 9(a), except that the seal actually lies flat against the overhang when m_s is negative in the discussed deflection range. Except when a sealed-gap width of 0.5 is used, the slopes of the seal-moment curves at small positive values of deflection are usually positive and indicate an increasing balancing effect in this range. This increase in balancing effect is independent of that obtained by the increased pressure difference across the balance when the flap is deflected or when the angle of attack of an airfoil is increased and is a function of the seal. At high positive values of overhang deflection, as the seal became taut, the seal-moment ratio of the unrestricted seal decreased and became negative and the direction of its force was opposite to that of the overhang balancing force (figs. 3(d) and 10(c)).

Effect of the Balance Configuration on the Seal-Moment Characteristics

Effect of seal width.- The effect on the seal-moment characteristics of varying the seal width, with other variables kept constant, is shown in figure 35 and is also evident from figures 14 to 19, 22 to 24, and 27 to 32. For a given sealed-gap width, m_s depends on seal width. The curves indicate that m_s decreases in the negative deflection range and generally at small positive deflections and usually increases at large positive deflections as the seal width increases. The curves indicate also that, for a given sealed-gap width and as the seal width increases, the maximum value of m_s generally increases, except when the circular backplate is used, and the maximum value of m_s occurs at an overhang deflection that increases with seal width, regardless of the backplate.

Effect of sealed-gap width.- The effect of sealed-gap width on seal-moment characteristics is indicated in figure 36 and in figures 14 to 19, 22 to 24, and 27 to 32. For a given seal width, the seal-moment ratio generally increases with sealed-gap width at small deflections and decreases at large deflections.

Effect of backplate.- The seal-moment characteristics obtained with the three backplates for given sealed-gap and seal widths generally differ only in the deflection range in which the seal lies against the backplate; hence the values of m_s in this range depend on the type of backplate contacted and the effect this backplate has on the seal profile. A comparison of the seal moments obtained over the deflection range with constant gaps and seals for the three different backplate arrangements is given in figure 37 for the condition in which no vertical restrictions are used. The characteristics exhibited by the seal with a vertical backplate and a circular backplate are quite similar (see also figs. 14 to 21 and 22 to 25) and indicate some linearity over a part of the deflection range. The horizontal backplate has little or no effect on the moments produced by the seal; these moments are usually larger at small deflections and smaller at large deflections than those obtained with the circular or vertical backplate. The effect of the backplate appears to diminish with an increase in size of the sealed gap and the seal, and the characteristics obtained with the three backplates differ by only a small amount with medium and large gaps and seals (figs. 37 and 14 to 34). At small gaps, the effect of a backplate constraining the seal is to cause the maximum moment of the seal to be reduced and to be developed at a higher deflection (fig. 37(a)).

Effect of vertical restriction.- Limiting the height of the balance chamber reduced the values of m_s over that part of the deflection range in which the seal contacted the roof of the chamber (figs. 11 and 14 to 34). Increasing the seal width or the overhang deflection in this condition or decreasing the value of the limiting overhang deflection δ_{b_l} caused a greater reduction in m_s as more of the seal contacted both the chamber ceiling and the backplate. The deflection at which the seal contacted the chamber ceiling and the seal moment started to decrease was greater with the horizontal backplate

than with the two other types tested. When no vertical restriction was present, the maximum values of m_s usually occurred at higher values of overhang deflection and the values of m_s were greater over the deflection range affected than when a restriction was used to simulate the roof of the balance chamber. It appears, therefore, that an optimum balance configuration would employ a seal width such that the seal would barely touch the chamber ceiling when maximum deflection is attained. (See figs. 5 and 8.)

Off-center seal attachment.- The seal-moment characteristics obtained with a $0.34c_b$ off-center attachment of the seal to the backplate are shown in figures 20, 21, 25, 26, 33, and 34 when tested with the three types of backplate used in the investigation. (The value of $0.34c_b$ of the off-center seal attachment corresponds to an offset of the position of seal attachment to the backplate to the top or bottom of the balance chamber when $\delta_{b_l} = 20°$.) In addition, a comparison of the seal-moment characteristics obtained in the presence of the circular backplate with the seal attached to the wing structure at the center and off-center positions is shown in figure 25. The seal-moment characteristics obtained with the off-center seal attachment were generally unfavorable over the deflection range because a decreasing balancing tendency or an increasing unbalancing tendency is indicated, regardless of the type of backplate or of the point of attachment. When attached above center, the seal invariably lay against the backplate and overhead restriction at positive deflections (figs. 7 and 12); when attached below center (figs. 6 and 13), however, the seal had a moment vector that would decrease positively, then increase negatively with overhang deflection. These effects account for the unbalancing characteristics of this type of seal attachment.

The effect of attaching the seal off center to a circular backplate when the seal did not contact the balance-chamber ceiling was to shift the seal-moment curve by an angle the sine of which was equal to the off-center displacement (expressed as a fraction of the overhang) divided by the radius of the backplate arc (also expressed as a fraction of the overhang). The curves of figure 25 approximately verify this conclusion; the computed offset angle was $\sin^{-1}\frac{0.34}{1.3} = 15.2°$, and

the data of figure 25 indicate that the offset angle is about 16°. Since an off-center seal attachment produces an unbalancing effect that may be greater than the increased balancing effect on the overhang caused by flap deflection or the increase in the angle of attack, this type of seal attachment is believed to be undesirable and should be avoided.

Comparison of Analytical and Experimental Seal-Moment Characteristics

The similarity between the analytical (reference 2) and experimental seal-moment characteristics is evident in figure 37, which shows the agreement between these results. The analytical and experimental results were compared for several configurations in addition to those herein and similar agreement was obtained.

Computation of Seal-Moment Characteristics by Approximate Method

The seal-moment ratio computed by the approximate method (reference 1) for various sizes of sealed gap is shown in figure 38. This method of computing the seal-moment ratio is independent of the seal width and assumes a balance chord equal to the overhang chord plus one-half the width of the sealed gap measured when the flap is in the neutral position. The inaccuracy of this method is apparent by a comparison of the values shown in figure 38 with the data of figures 14 to 34. As indicated in reference 2, the error involved in using the approximate method may be a considerable part of the hinge-moment coefficient or control force of the balanced control surface; it is therefore believed that this method should not be used.

Application of Seal-Moment Data

Inasmuch as the investigation reported herein was made with the various limitations and configurations of an internal-balance arrangement and the data presented are representative of the seal effects in such configurations, the figures are believed to be applicable for design purposes in calculating the hinge-moment characteristics of various balanced flaps with thin-plate overhangs,

if the pressure difference across the balance and the plain-flap hinge-moment coefficients are known. In order to obtain the seal characteristics of those configurations not tested, it is possible to interpolate between the seal-moment curves for an intermediate gap or seal-width configuration. As indicated in reference 2, these results are believed to be applicable also to overhangs having nose shapes with fairly small angles, but the limiting nose angle has not yet been determined.

EXAMPLES

Comparison of experimental and computed hinge-moment coefficients of a balanced flap.- The aileron configurations shown in figure 39 were selected to illustrate the computations necessary for a practical application of the seal-moment data to the balancing moment of an internally balanced flap. The plain-sealed-flap hinge-moment data for the 0.20c aileron were used in the computations, together with the pressure coefficient across the balance P_R (from unpublished data) given in figure 40, the seal-moment data presented herein, and the geometric dimensions of the balance. In figure 40, the computed balanced-aileron hinge-moment coefficients are compared with the balanced-aileron hinge-moment coefficients obtained experimentally.

The computed balancing moments were obtained by the following equation, which is based on the geometric dimensions of the balance arrangement for a unit span (two-dimensional):

$$\Delta c_{h_a} = \frac{P_R}{2}\left[\left(\frac{c_b}{c_a}\right)^2 (1 + m_s) - \left(\frac{t/2}{c_a}\right)^2\right]$$

$$= \frac{P_R}{2}\left[(0.744)^2(1 + m_s) - (0.1875)^2\right]$$

$$= \frac{P_R}{2}\left[0.553(1 + m_s) - 0.0352\right]$$

Values of P_R for use in this equation were obtained from figure 40. The width of the seal used in the investigation was not measured but was believed to have been approximately 0.4. Values of m_s for computing the exact balancing moment over the deflection range for a seal width of 0.4 and a sealed-gap width of 0.0336 were interpolated from the data of figure 22 and figures 14 and 15. (The characteristics of the seals with vertical and circular backplates are somewhat similar at this seal width and sealed-gap width.)

The balanced-aileron hinge-moment coefficients were obtained by the equation

$$c_{h_a}{}_{\text{balanced aileron}} = c_{h_a}{}_{\text{plain aileron}} + \Delta c_{h_a}$$

and figure 40 shows fair agreement between experimental and computed results. The discrepancy between the balanced-aileron characteristics obtained experimentally and those computed is probably caused by the difference in the size of the vent gap (0.005c for plain aileron, 0.010c for balanced aileron) and by possible small differences in model configuration such as seal width, chord of overhang, and thickness of overhang.

Comparison of the computed balanced-flap hinge-moment coefficients with and without balance-chamber restrictions.- A comparison of the computed balanced-flap hinge-moment coefficients, with curves showing the effect of the vertical chamber restriction either neglected or considered, is presented in figure 41 to illustrate the type of balanced-flap hinge-moment coefficient that would be obtained if a very wide seal were used in a configuration of an internally balanced aileron. For these computations, an overhang chord of $0.52c_a$, a seal width of 0.6, $\delta_{b_l} = 21^\circ$, and a sealed-gap width of 0.1 (values of m_s obtained from figure 22(c)) were assumed installed on the plain sealed aileron of figure 39 and the other data, supplied in figures 39 and 40, were assumed to remain the same. (See fig. 41.) The method of computation was the same as that previously outlined. Neglecting the effect of the vertical balance-chamber restriction (that is, with no limiting value for δ_b) results in

considerable error at large deflections, when the seal contacts the balance-chamber ceiling. (See fig. 41.) The optimum seal width would be such that the seal would barely touch the chamber ceiling at the maximum overhang deflection (see section entitled "Effect of vertical restriction") and, for this aileron configuration, figure 22 indicates that a seal width of about 0.5 would be optimum. Up to deflections of $\pm 18^\circ$, the curve for aileron-hinge-moment coefficients computed for $s = 0.5$ and $\delta_{b_l} = 21^\circ$ is approximately the same as that shown in figure 41 for $s = 0.6$ and no limiting value for δ_b; for deflections beyond $\pm 18^\circ$, this curve is almost parallel to the curve shown in figure 41 for $s = 0.6$ and $\delta_{b_l} = 21^\circ$.

The error involved in the use of the approximate method is also illustrated in figure 41: the approximate method indicates that the seal contributes more balancing moment than that actually produced over almost the entire deflection range.

CONCLUSIONS

As an experimental verification and an extension of a previous analytical investigation, tests were made to determine the hinge moments produced in an internal-balance arrangement by fabric seals of various widths that seal flap-nose gaps of various widths in the presence of a thin-plate overhang. The tests were conducted with horizontal, vertical, and circular types of balance-chamber wall forward of the balance and with various heights of the balance chamber. The investigation indicated the following conclusions:

1. The moment of the seal may be a balancing or an unbalancing moment and may be an appreciable part of the total balancing moment of an internally balanced flap, depending on the overhang deflection and the configuration of the internal balance.

2. Variation of the width of the seal, the sealed gap, or the location of the seal attachment to the wing structure affected the seal moments through most of the overhang deflection range.

3. The shape and size of the balance chamber affected the seal-moment characteristics in the deflection range at which the seals contacted and were constrained by the chamber walls; the values of the seal moments were usually reduced when the seals were constrained.

4. An optimum balance configuration employs a seal width such that the seal barely touches the chamber ceiling when maximum overhang deflection is attained.

Langley Memorial Aeronautical Laboratory
National Advisory Committee for Aeronautics
Langley Field, Va.

REFERENCES

1. Rogallo, F. M., and Lowry, John G.: Résumé of Data for Internally Balanced Ailerons. NACA RB, March 1943.

2. Murray, Harry E., and Erwin, Mary A.: Hinge Moments of Sealed-Internal-Balance Arrangements for Control Surfaces. I - Theoretical Investigation. NACA ARR No. L5F30, 1945.

TABLE I.- BALANCE CONFIGURATIONS TESTED

Location of seal attachment (fraction of c_b)	Width of sealed gap (fraction of c_b)	Width of seal (fraction of c_b)	δ_{b_l} (deg)	Figure
Vertical backplate				
Center of backplate	0	0.4	None, 15	14(a)
	0	.6	None, 16, 21, 26	14(b)
	.1	.4	None, 16	15(a)
	.1	.6	None, 16, 21, 26	15(b)
	.2	.5	None, 16	16(a)
	.2	.6	None, 16, 21	16(b)
	.2	.8	None, 16, 21, 26, 30	16(c)
	.3	.6	None, 16	17(a)
	.3	.8	None, 16, 21, 26	17(b)
	.4	.7	None, 16, 21	18(a)
	.4	.9	None, 16, 22, 26, 30	18(b)
	.5	.7	None, 16	19(a)
	.5	.9	None, 16, 21, 26	19(b)
0.34 above and below center of backplate	.3	.8	20	20
	.5	.9	20, 25	21
Circular backplate				
Center of backplate	0.1	0.4	None, 16	22(a)
	.1	.5	None, 16, 21	22(b)
	.1	.6	None, 16, 21, 25	22(c)
	.3	.6	None, 16, 20	23(a)
	.3	.7	None, 16, 21, 26	23(b)
	.3	.8	None, 16, 21, 25	23(c)
	.5	.7	None, 16	24(a)
	.5	.8	None, 16, 21	24(b)
	.5	.9	None, 16, 21, 25	24(c)
0.34 above and below center of backplate	.3	.8	20	25
	.5	.9	20, 25	26
Horizontal backplate				
Center of backplate	0	0.4	None	27(a)
	0	.6	None, 16	27(b)
	0	.8	None, 15, 20, 25	27(c)
	.1	.4	None	28(a)
	.1	.5	None, 16	28(b)
	.1	.7	None, 15, 20, 25	28(c)
	.1	.9	None, 25, 30	28(d)
	.2	.5	None, 16	29(a)
	.2	.7	None, 15, 20, 25	29(b)
	.2	.9	None, 26, 31	29(c)
	.3	.6	None, 16	30(a)
	.3	.7	None, 15, 20	30(b)
	.3	.9	None, 25, 31	30(c)
	.4	.6	None, 16	31(a)
	.4	.7	None, 15, 20	31(b)
	.4	.9	None, 16, 21, 25	31(c)
	.5	.7	None, 15	32(a)
	.5	.9	None, 16, 20, 26	32(b)
0.34 above and below center of backplate	.1	.7	20	33
	.5	.9	20,26	34

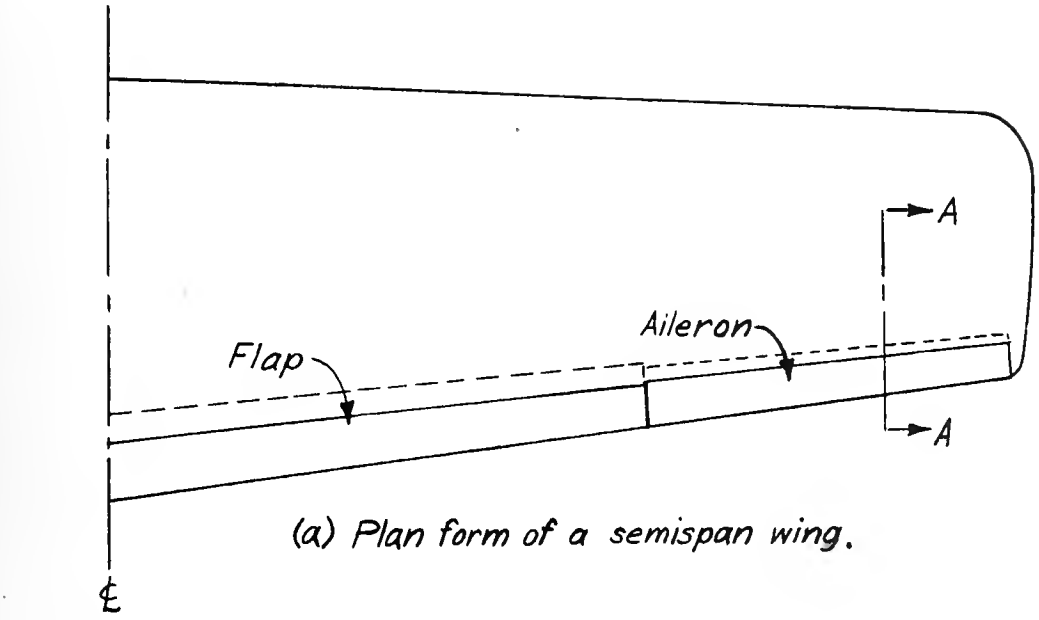

(a) Plan form of a semispan wing.

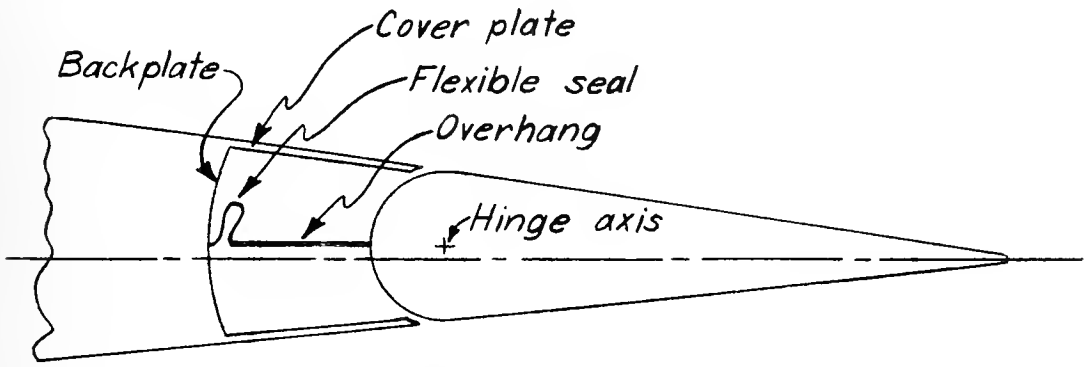

(b) Section A-A.

NATIONAL ADVISORY
COMMITTEE FOR AERONAUTICS

Figure 1.- Schematic diagram of a typical internal-balance arrangement for an aileron on a tapered wing.

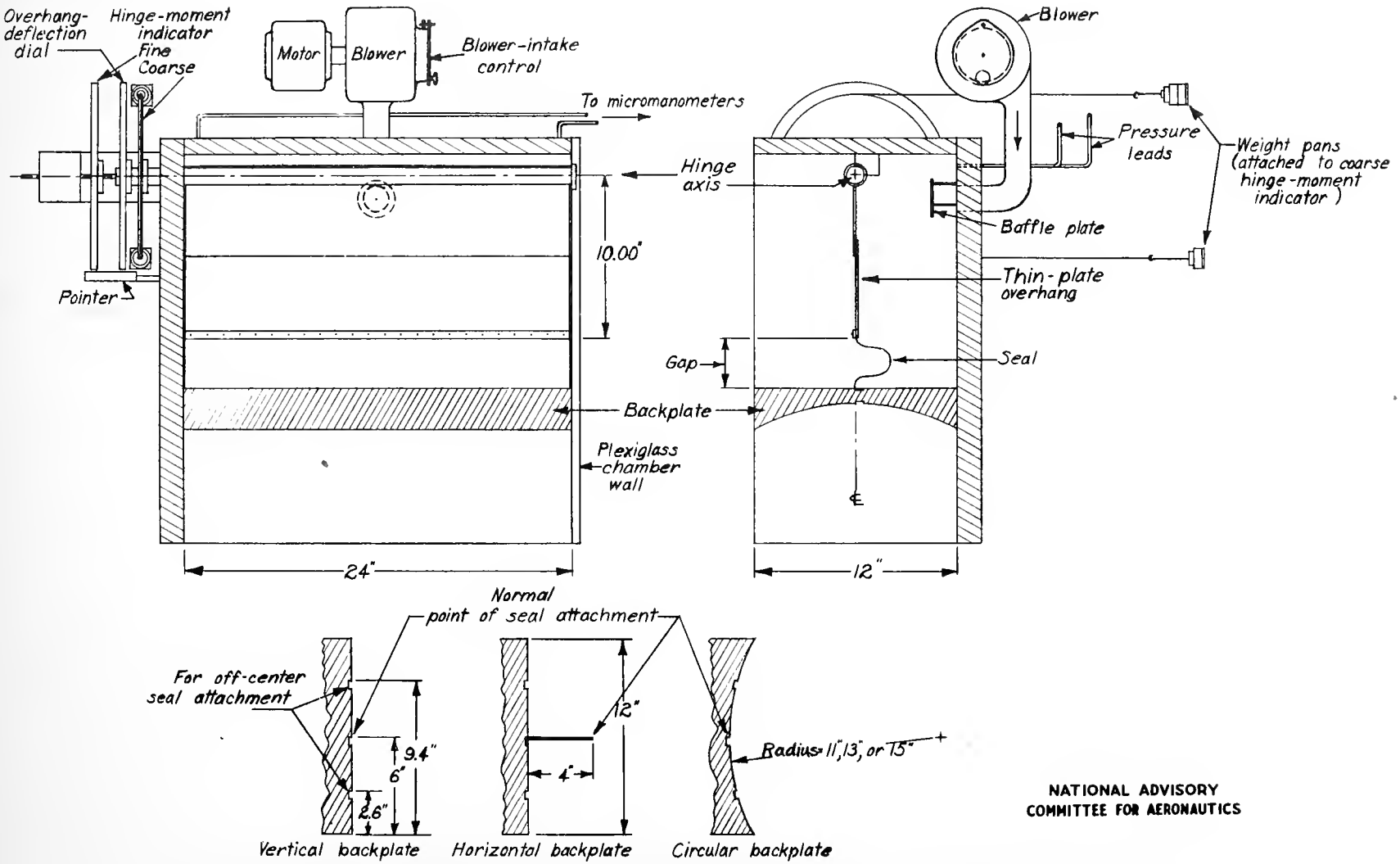

(a) Schematic diagram of testing apparatus and the three types of backplates used.

Figure 2.-Test setup.

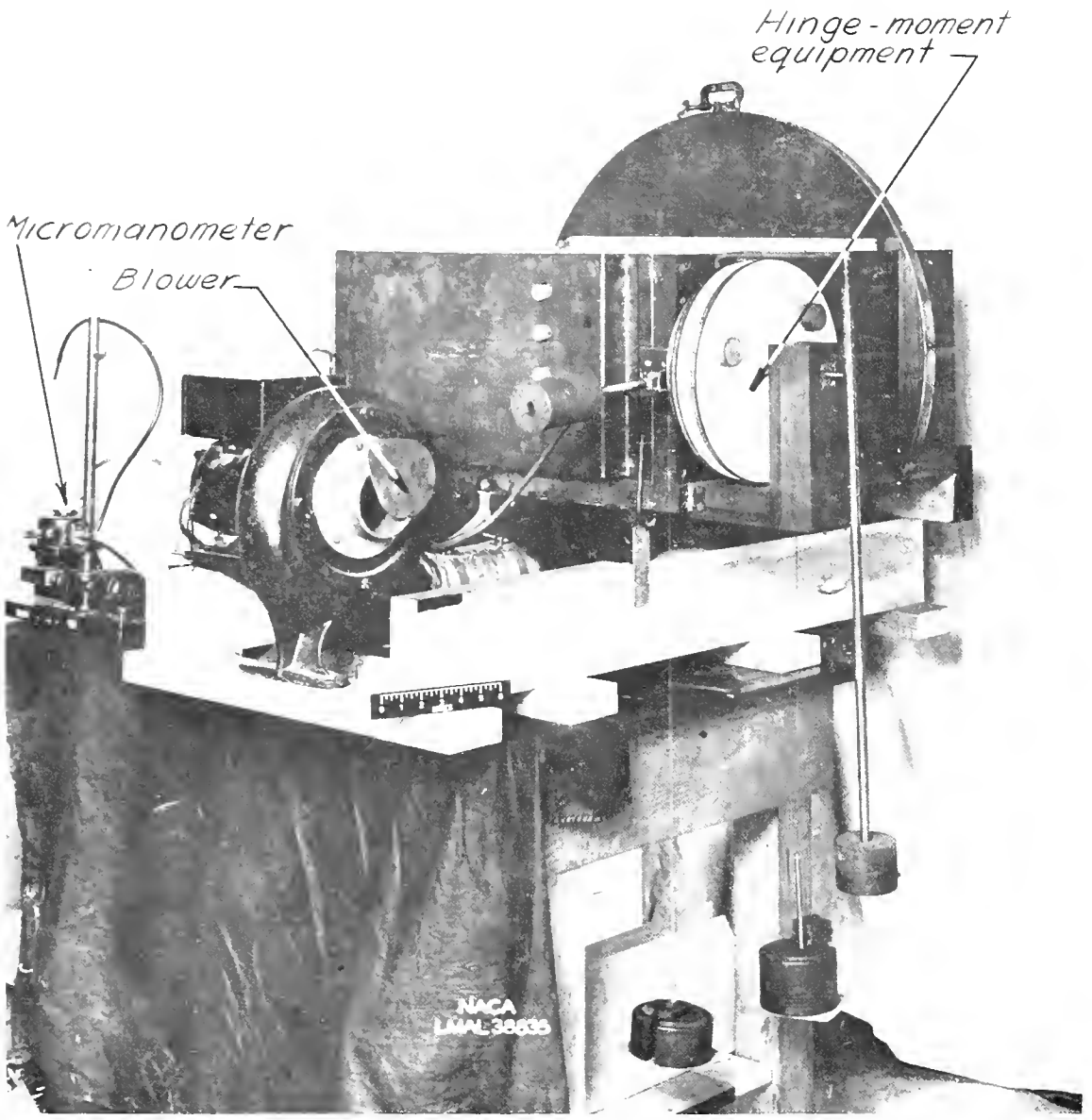

Figure 2(b).- Three-quarter rear view of testing apparatus.

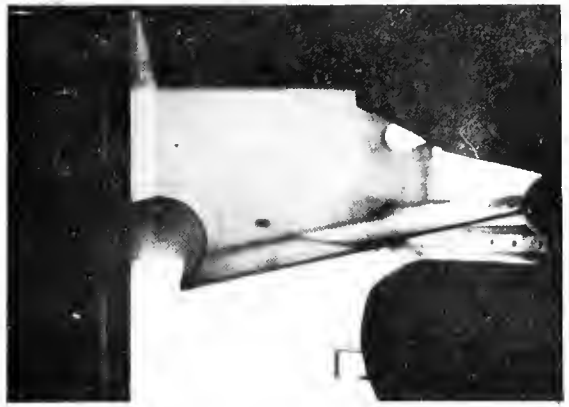

(a) $\delta_b = -12^\circ$.

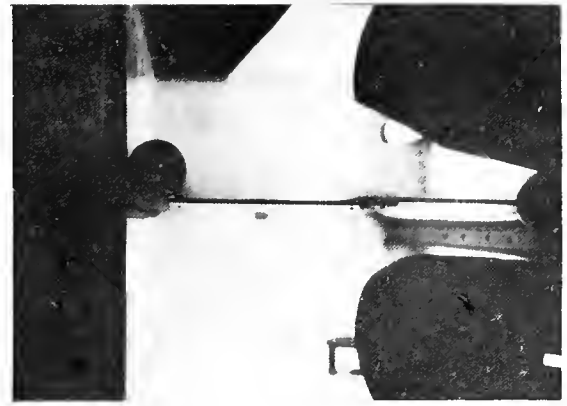

(b) $\delta_b = 0^\circ$.

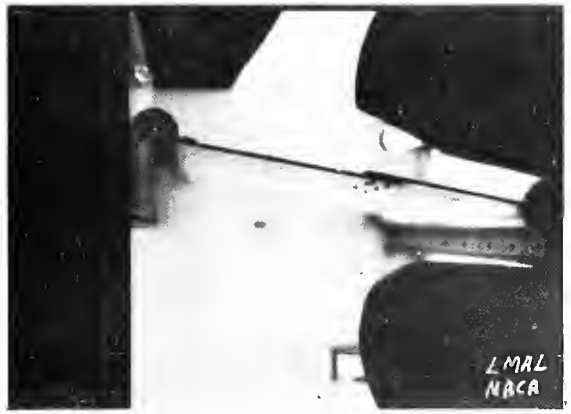

(c) $\delta_b = 10^\circ$.

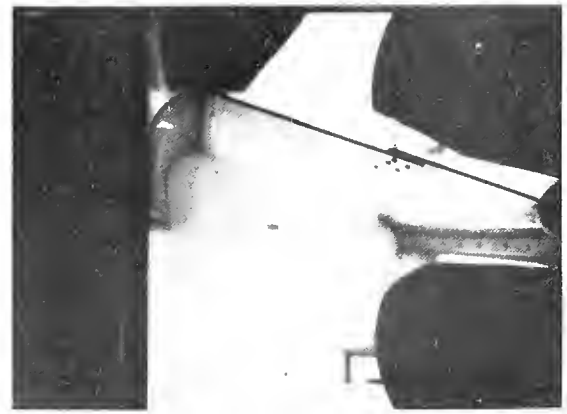

(d) $\delta_b = 18^\circ$.

Figure 3.- Seal test apparatus with vertical backplate. s = 0.4; g = 0.1.

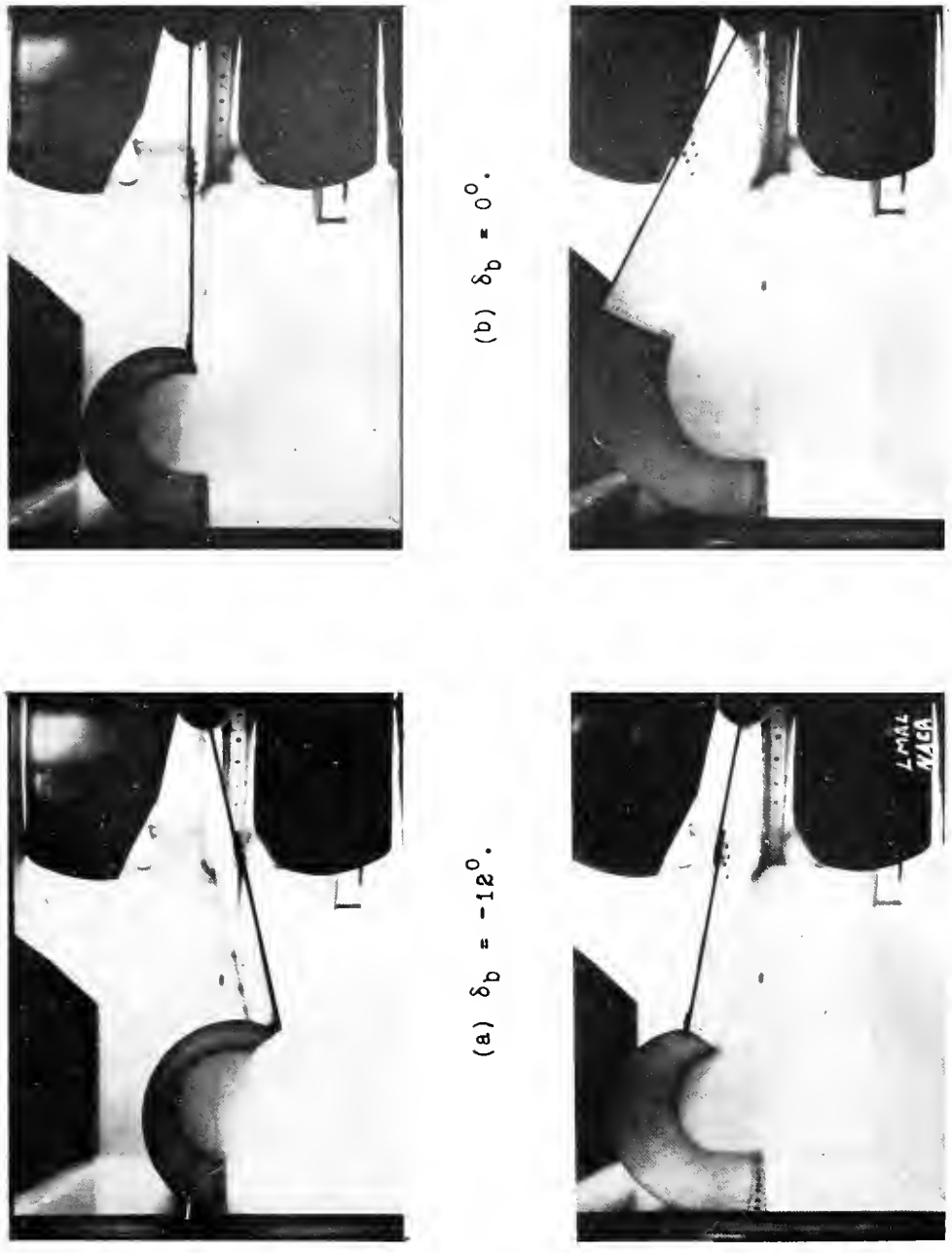

(a) $\delta_b = -12^\circ$. (b) $\delta_b = 0^\circ$. (c) $\delta_b = 10^\circ$. (d) $\delta_b = 26^\circ$.

Figure 4.- Seal test apparatus with vertical backplate. s = 0.8; g = 0.6.

Figure 5.- Seal test apparatus with vertical backplate. $s = 0.4$; $g = 0.1$; $\delta_b = 15^\circ$; $\delta_{b_l} = 15^\circ$.

Figure 6.- Seal test apparatus with vertical backplate. Seal attached $0.34c_b$ below center. $s = 0.9$; $g = 0.5$; $\delta_b = 10^\circ$; $\delta_{b_l} = 25^\circ$.

Figure 7.- Seal test apparatus with vertical backplate. Seal attached $0.34c_b$ above center. $s = 0.9$; $g = 0.5$; $\delta_b = 10^\circ$; $\delta_{b_l} = 25^\circ$.

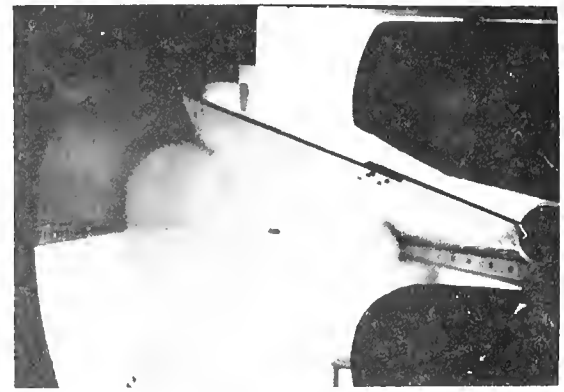

Figure 8.- Seal test apparatus with circular backplate. $s = 0.6$; $g = 0.3$; $\delta_b = 20^\circ$; $\delta_{b_l} = 20^\circ$.

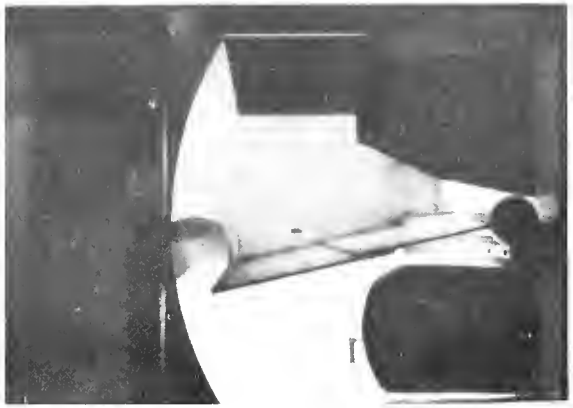

(a) $\delta_b = -12^\circ$.

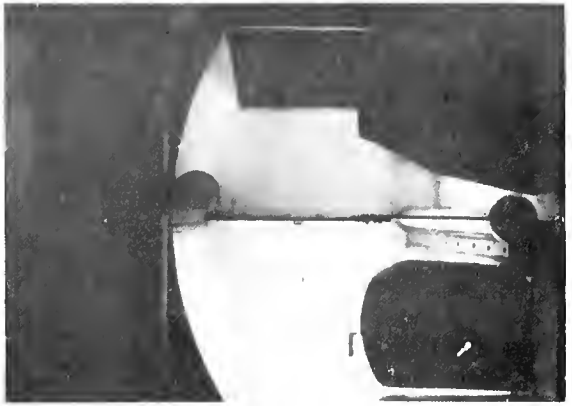

(b) $\delta_b = 0^\circ$.

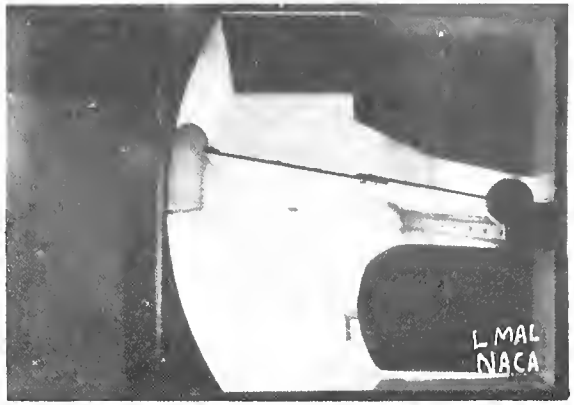

(c) $\delta_b = 10^\circ$.

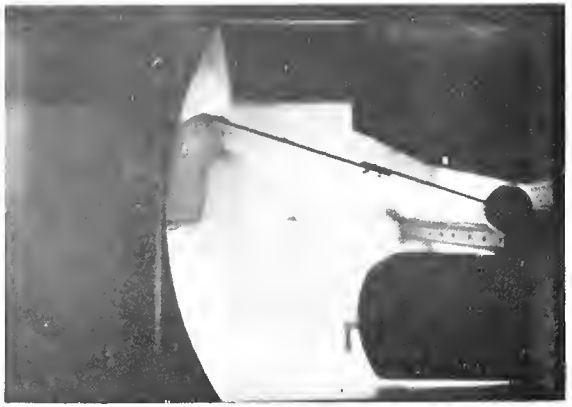

(d) $\delta_b = 18^\circ$.

Figure 9.- Seal test apparatus with circular backplate. s = 0.4; g = 0.1.

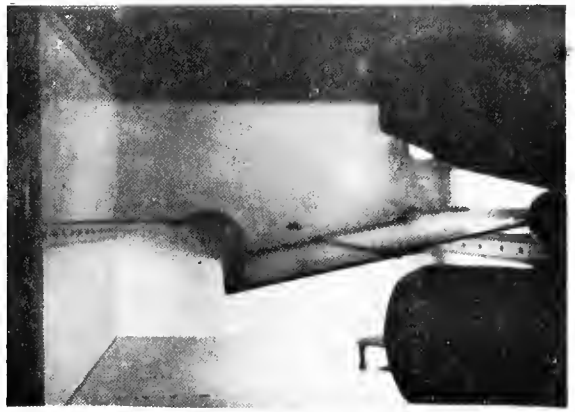

(a) $\delta_b = -12^\circ$.

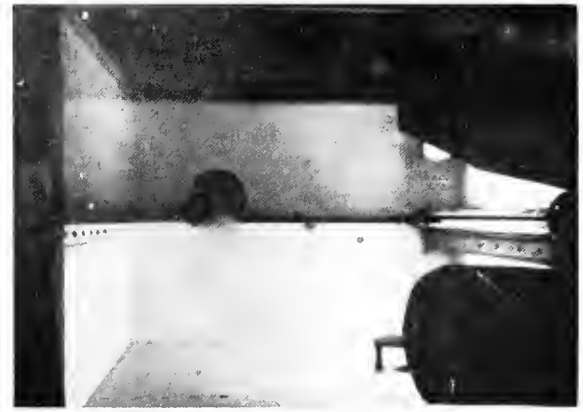

(b) $\delta_b = 0^\circ$.

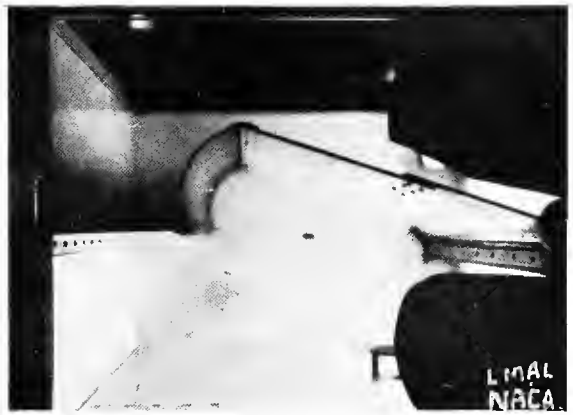

(c) $\delta_b = 18^\circ$.

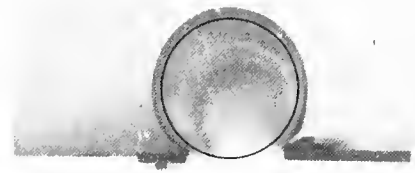

(d) Enlarged photograph of seal with circle superimposed to indicate circular shape of seal in presence of horizontal backplate. $\delta_b = 0^\circ$.

Figure 10.- Seal test apparatus with horizontal backplate. $s = 0.4$; $g = 0.1$.

(a) $\delta_b = 10^\circ$.

(b) $\delta_b = 20^\circ$.

Figure 11.- Seal test apparatus with horizontal backplate. $s = 0.9$; $g = 0.5$; $\delta_{b_l} = 20^\circ$.

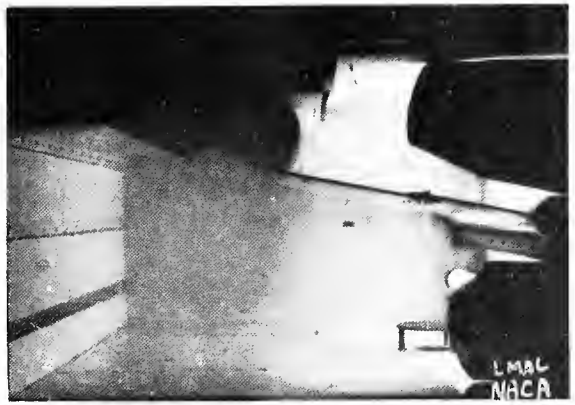

Figure 12.- Seal test apparatus with horizontal backplate. Seal attached $0.34c_b$ above center. $s = 0.9$; $g = 0.5$; $\delta_b = 10^\circ$; $\delta_{b_l} = 25^\circ$.

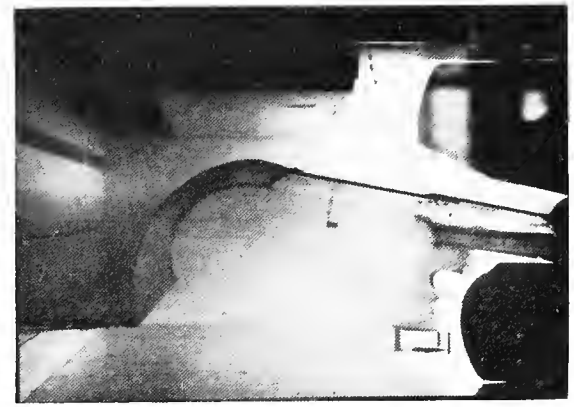

Figure 13.- Seal test apparatus with horizontal backplate. Seal attached $0.34c_b$ below center. $s = 0.9$; $g = 0.5$; $\delta_b = 10^\circ$; $\delta_{b_l} = 25^\circ$.

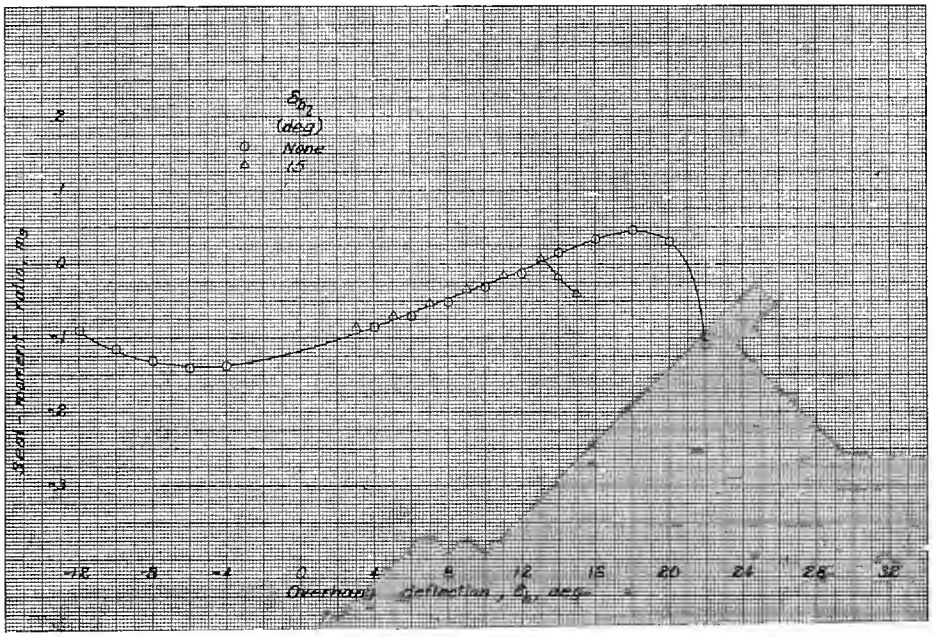

(a) s = 0.4.

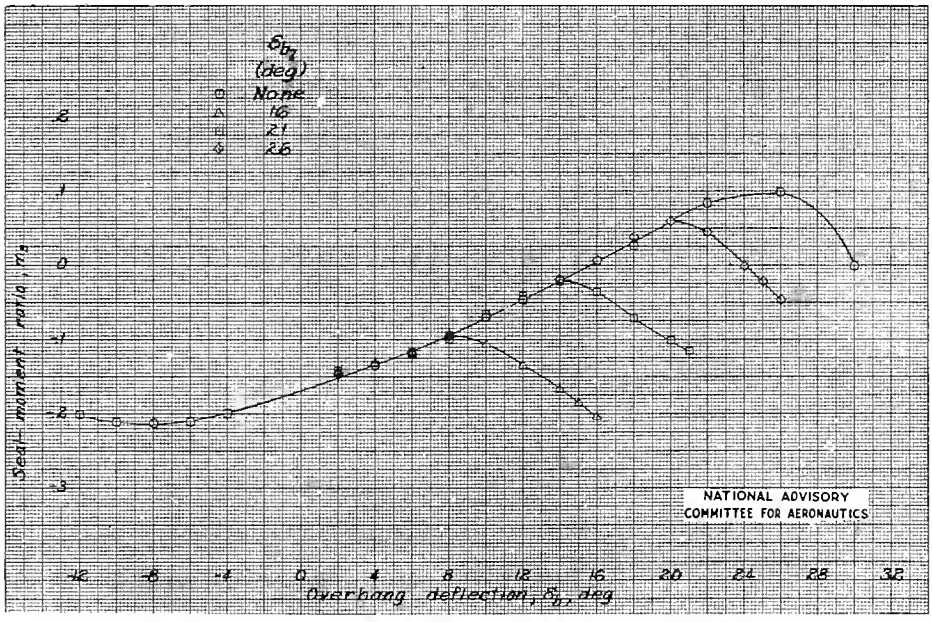

(b) s = 0.6.

Figure 14.- Hinge-moment characteristics of seals with vertical backplate. g = 0.

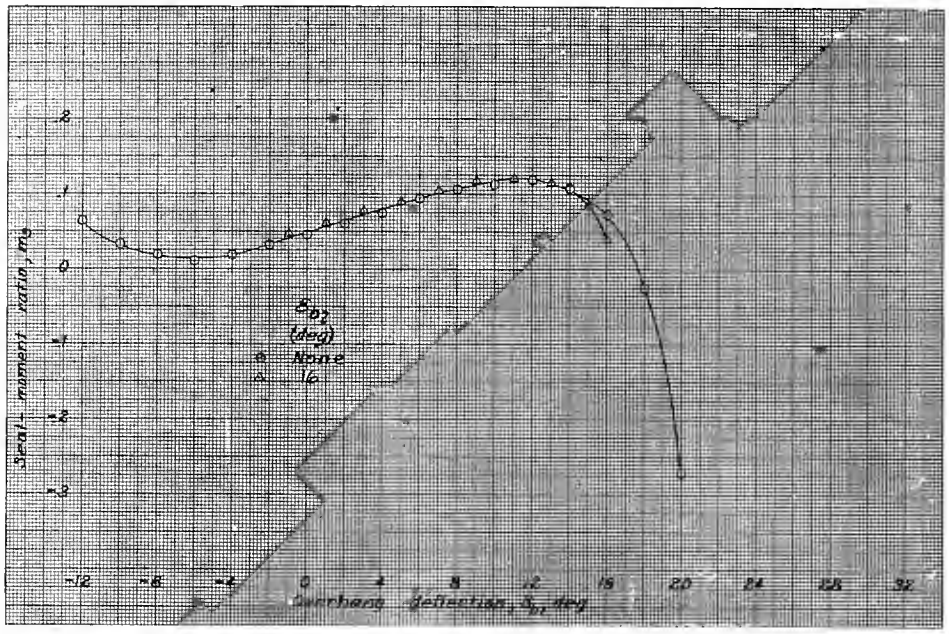

(a) s = 0.4.

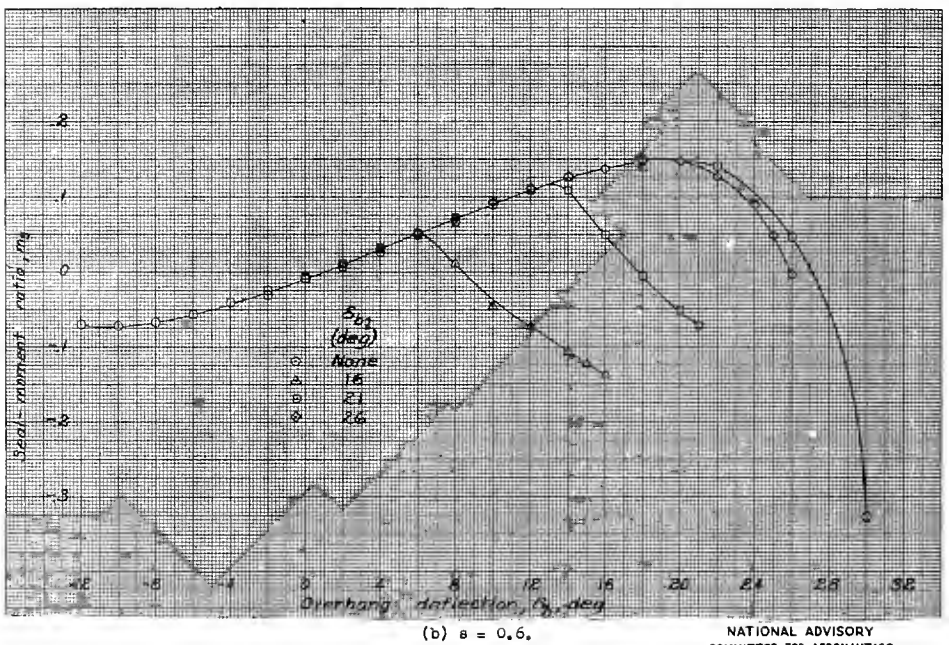

(b) s = 0.6.

NATIONAL ADVISORY COMMITTEE FOR AERONAUTICS

Figure 15.- Hinge-moment characteristics of seals with vertical backplate. S = 0.1.

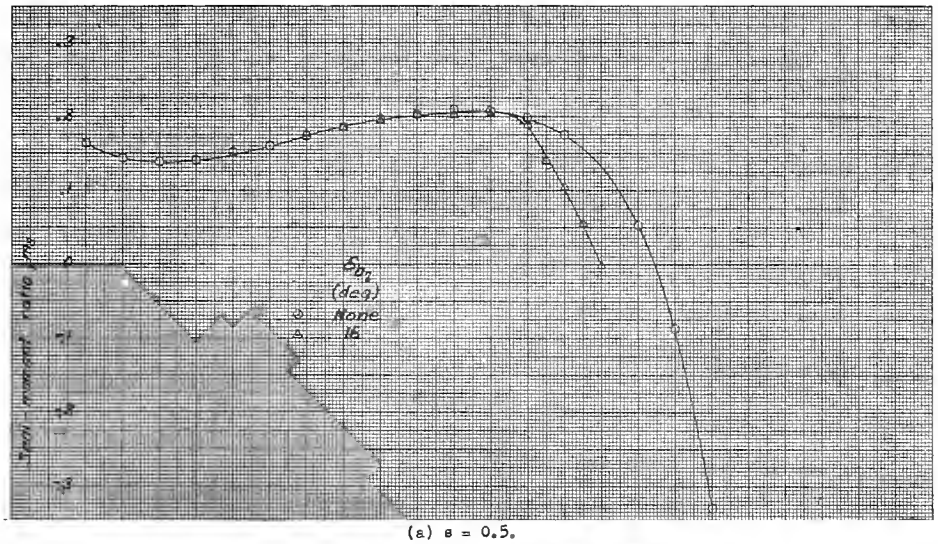

(a) s = 0.5.

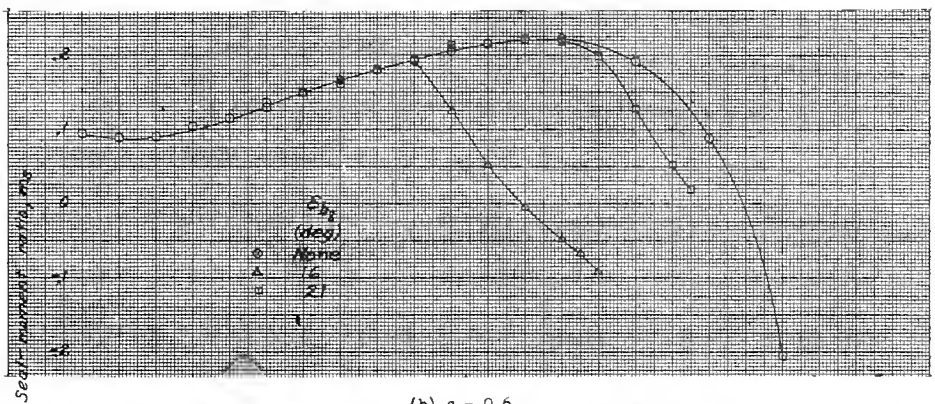

(b) s = 0.6.

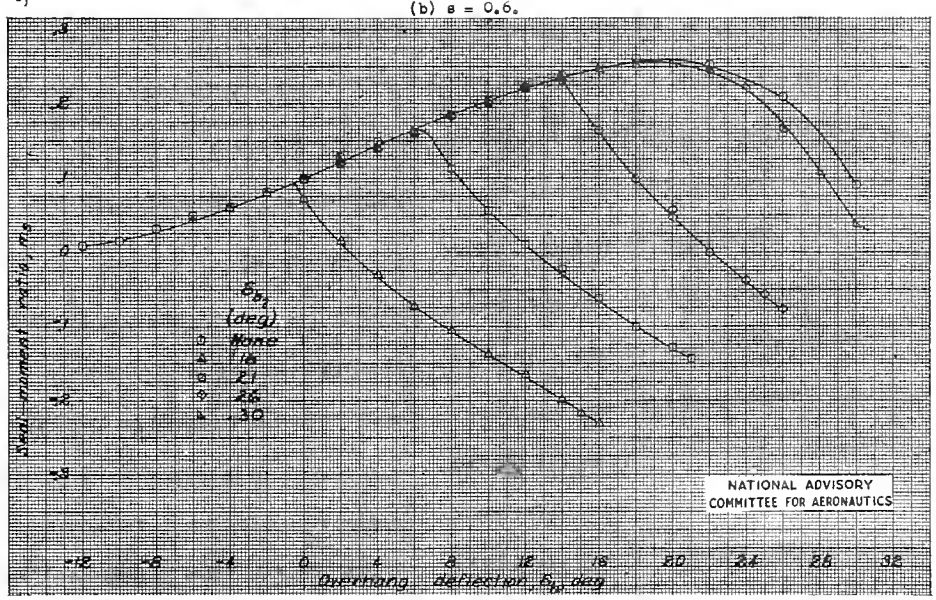

(c) s = 0.8.

Figure 16.- Hinge-moment characteristics of seals with vertical backplate. g = 0.2.

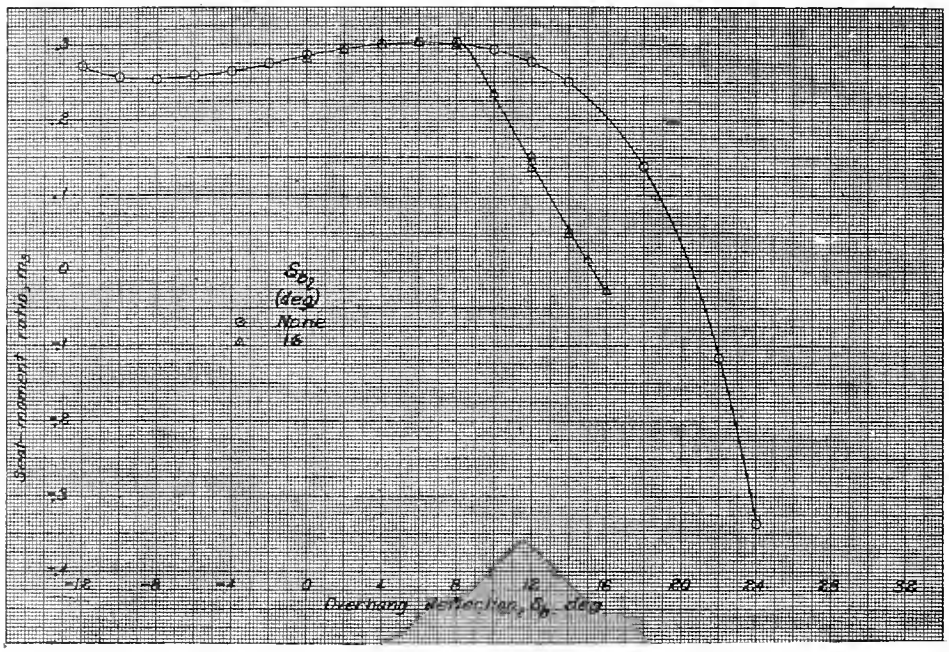

(a) s = 0.6.

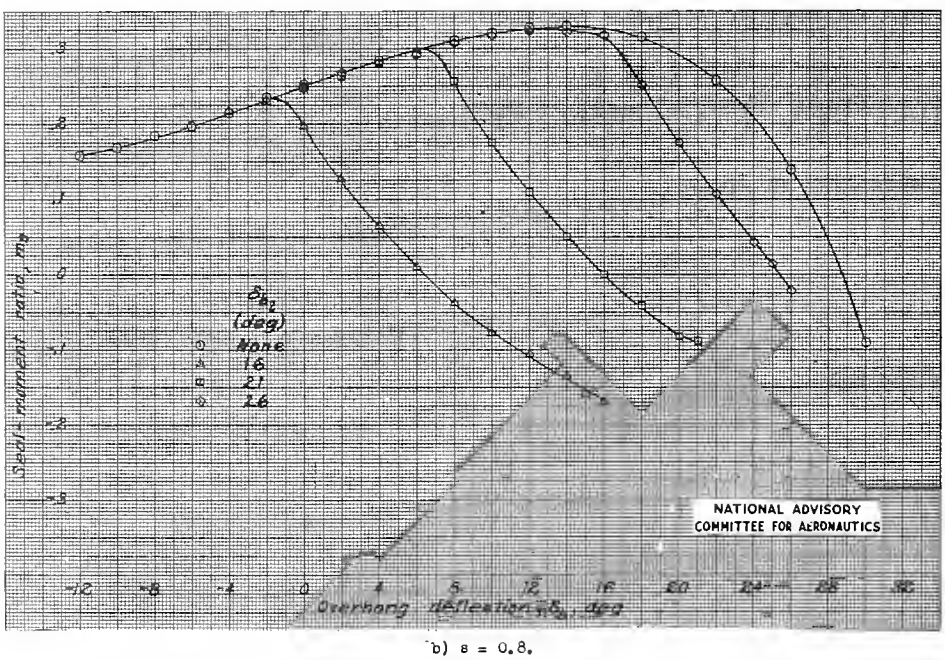

(b) s = 0.8.

Figure 17.- Hinge-moment characteristics of seals with vertical backplate, g = 0.3.

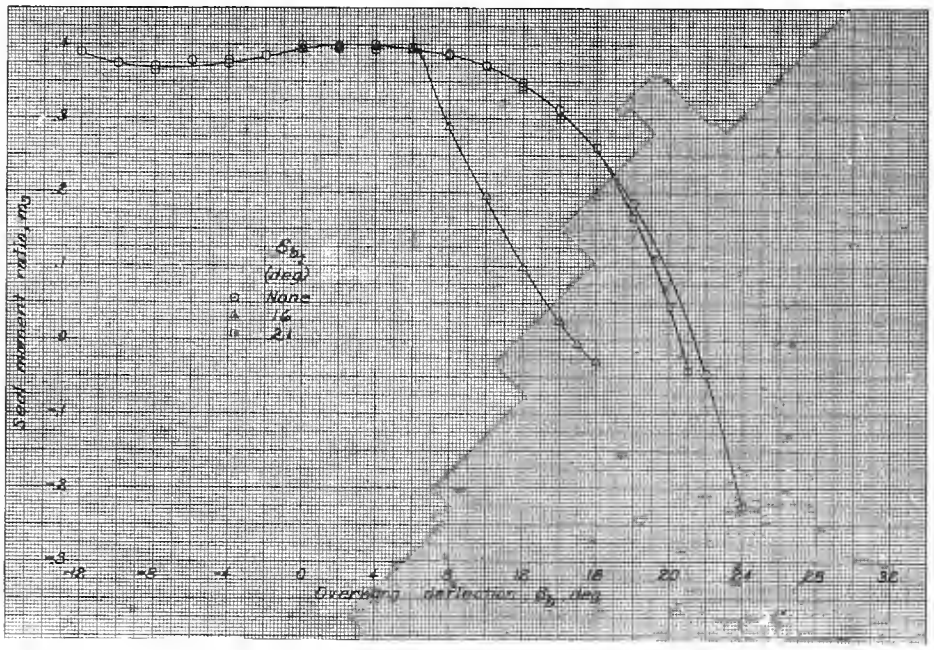

(a) s = 0.7.

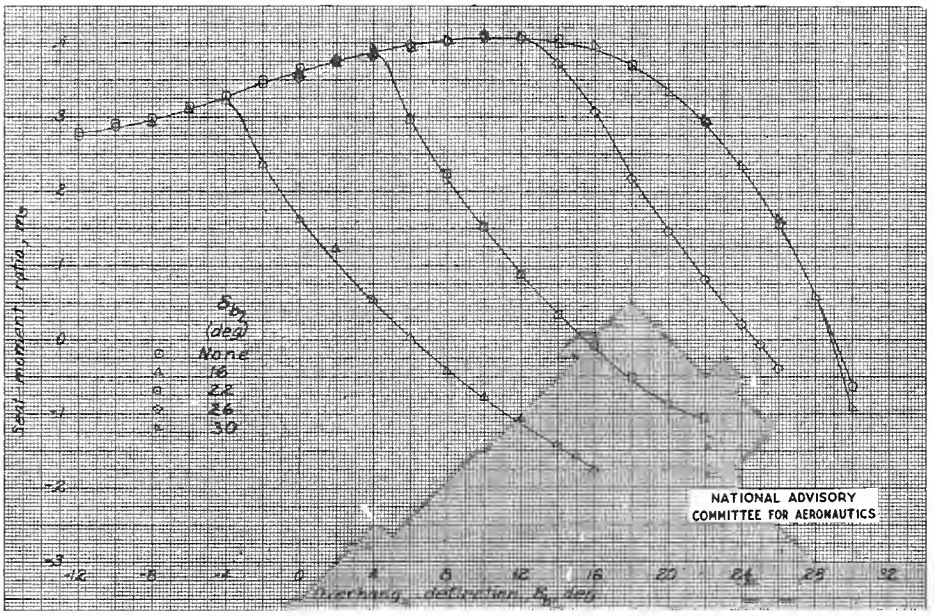

(b) s = 0.9.

Figure 18.- Hinge-moment characteristics of seals with vertical backplate.
g = 0.4.

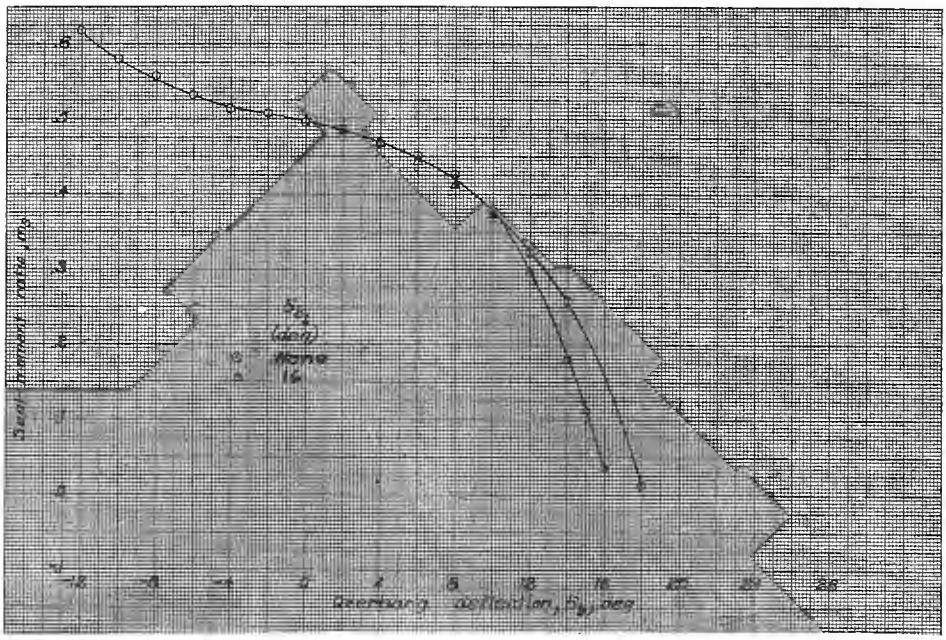

(a) $s = 0.7$.

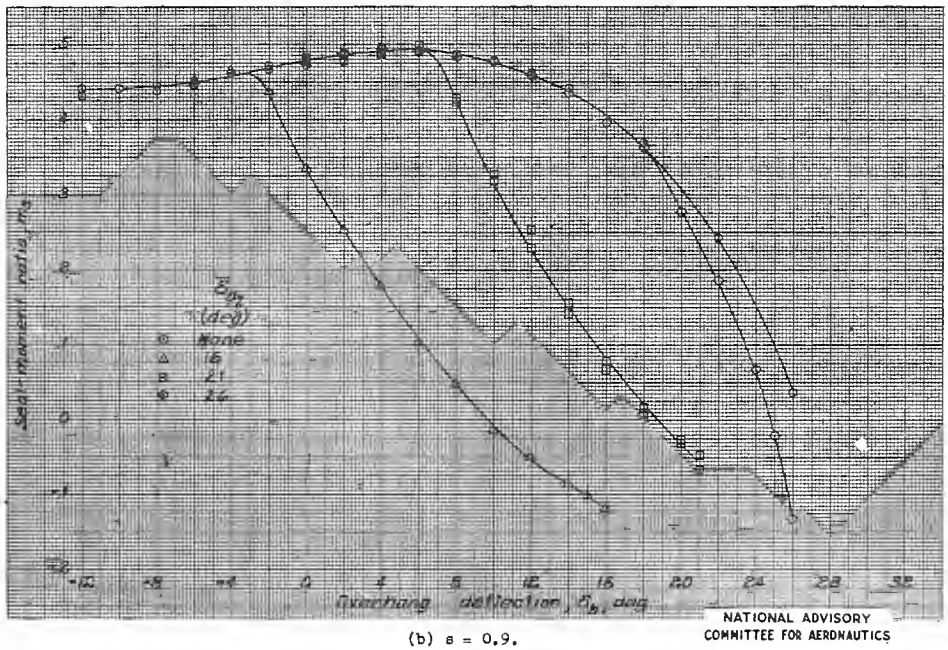

(b) $s = 0.9$.

Figure 19.- Hinge-moment characteristics of seals with vertical backplate. $\tau = 0.5$.

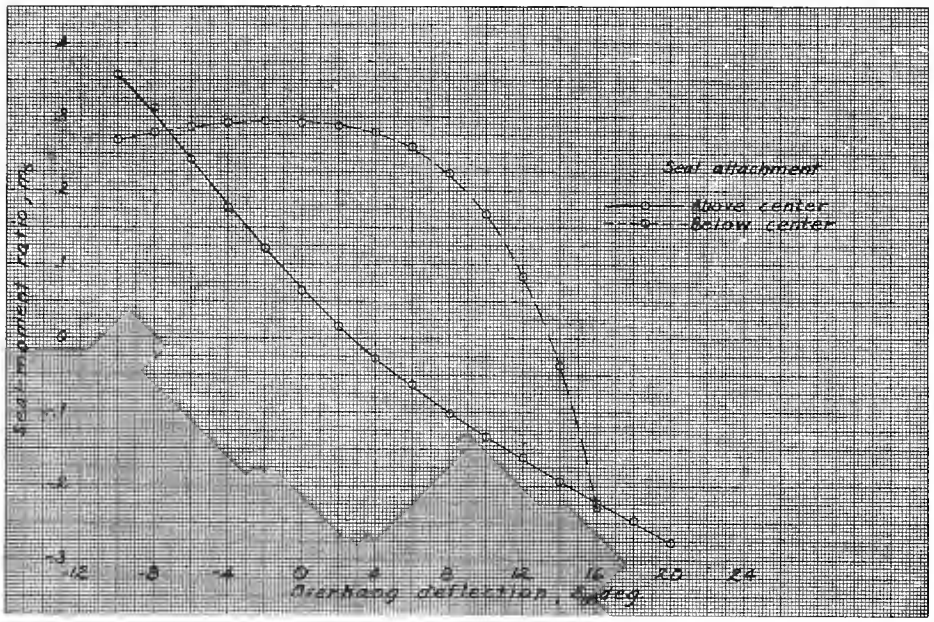

Figure 20.- Hinge-moment characteristics of seals attached $0.34c_b$ off center to vertical backplate. e = 0.8; g = 0.3; $\delta_{b_1} = 20°$.

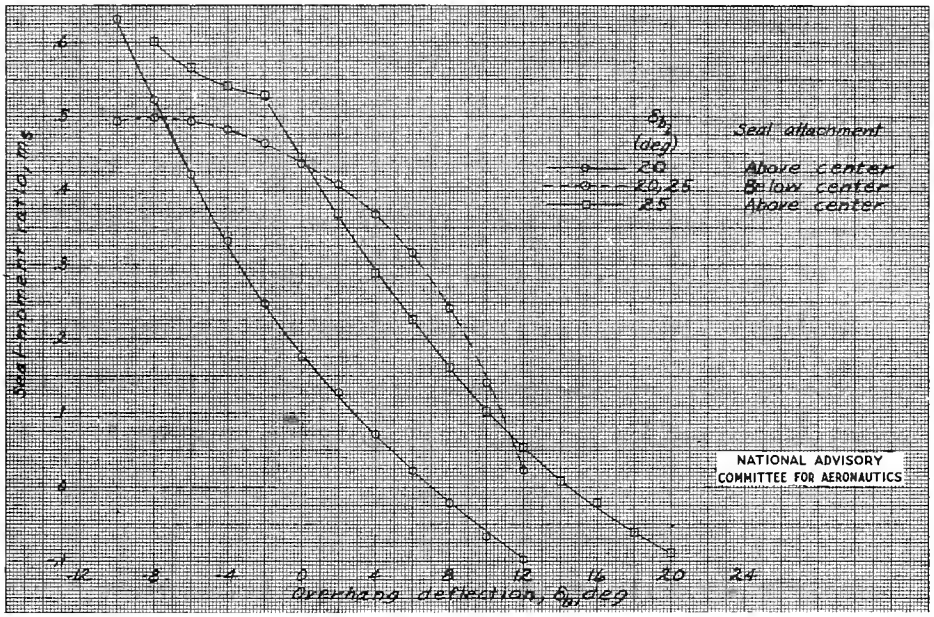

Figure 21.- Hinge-moment characteristics of seals attached $0.34c_b$ off center to vertical backplate. e = 0.9; g = 0.5.

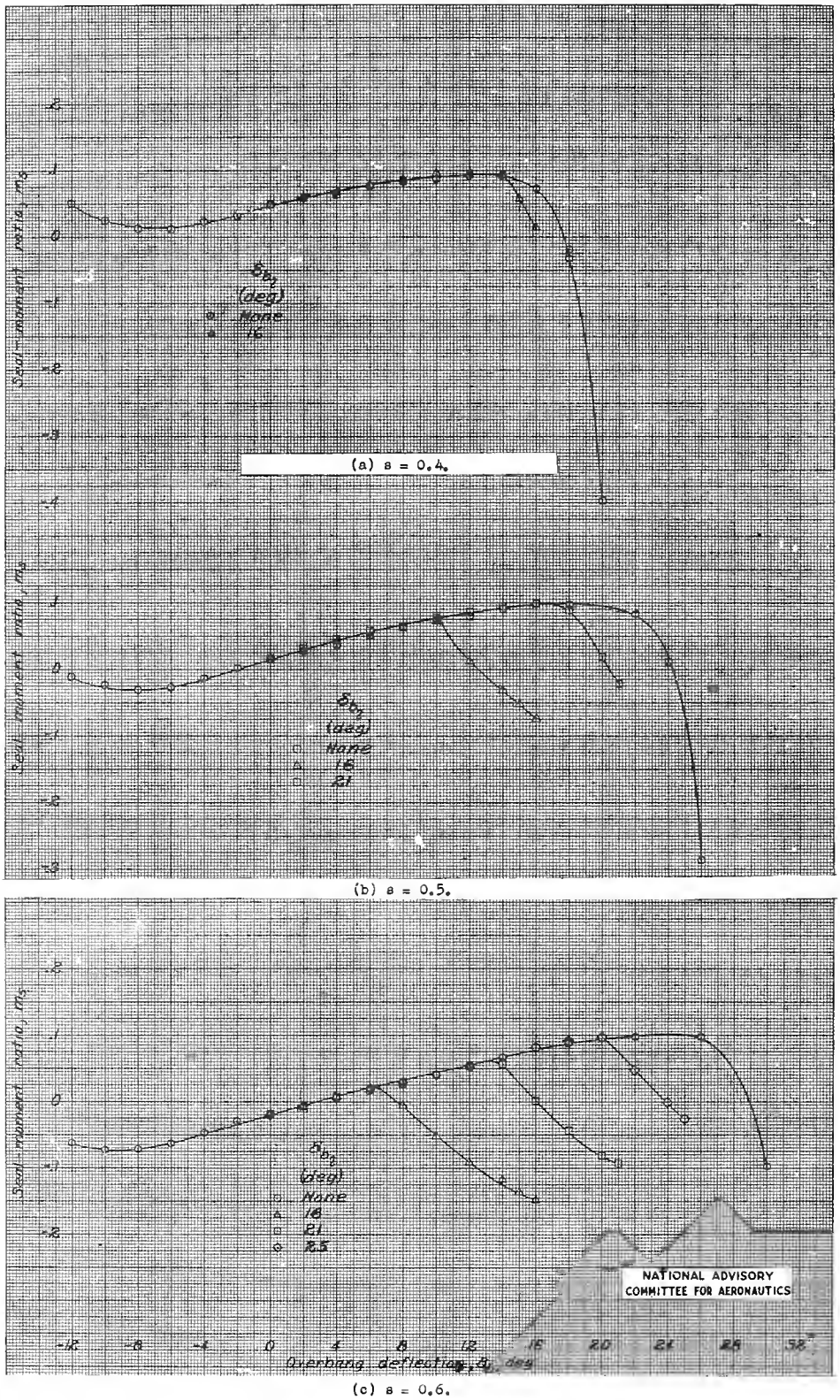

Figure 22.- Hinge-moment characteristics of seals with circular backplate. g = 0.1.

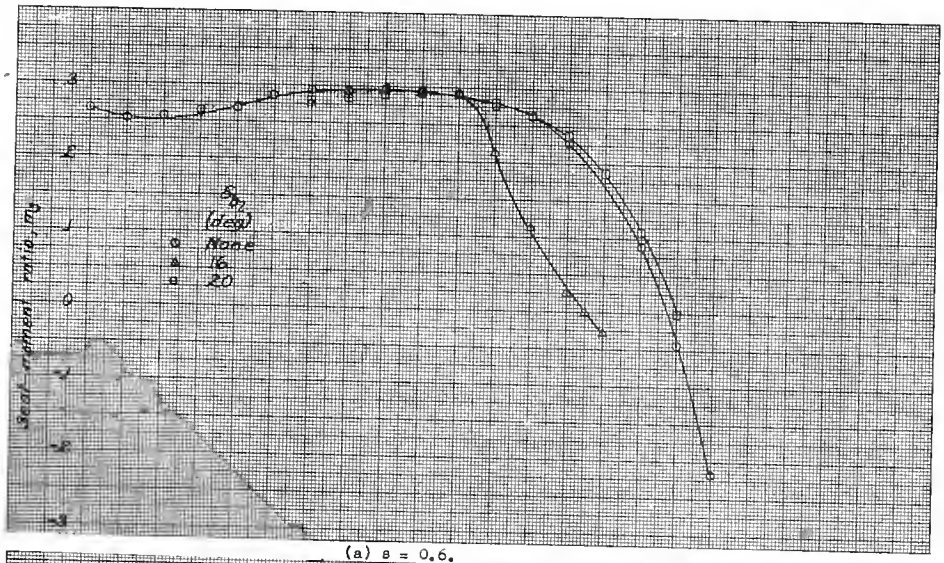

(a) $s = 0.6$.

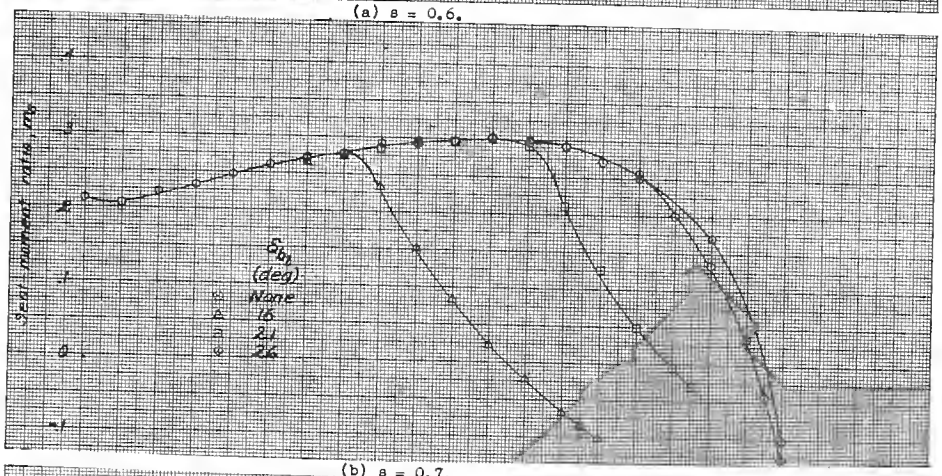

(b) $s = 0.7$.

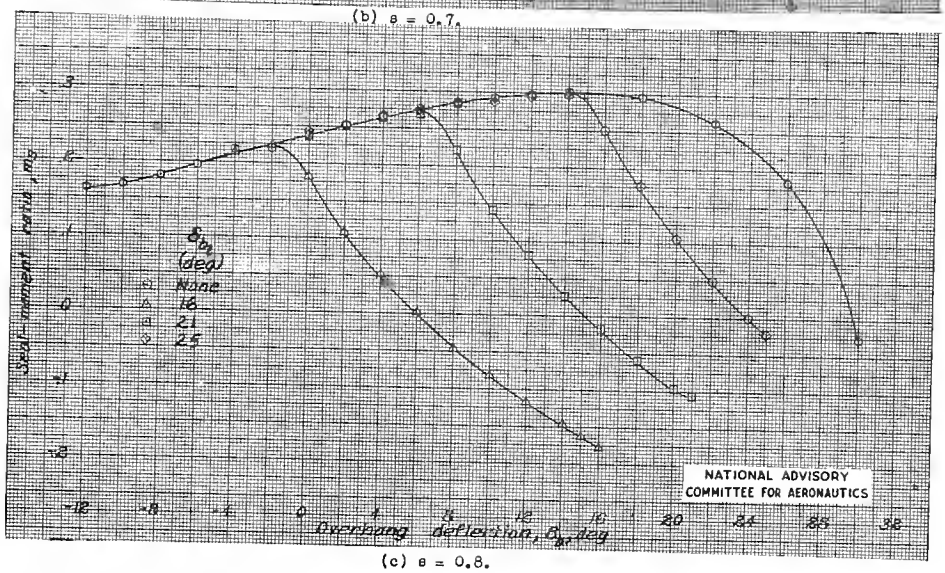

(c) $s = 0.8$.

Figure 23.- Hinge-moment characteristics of seals with circular backplate. $g = 0.3$.

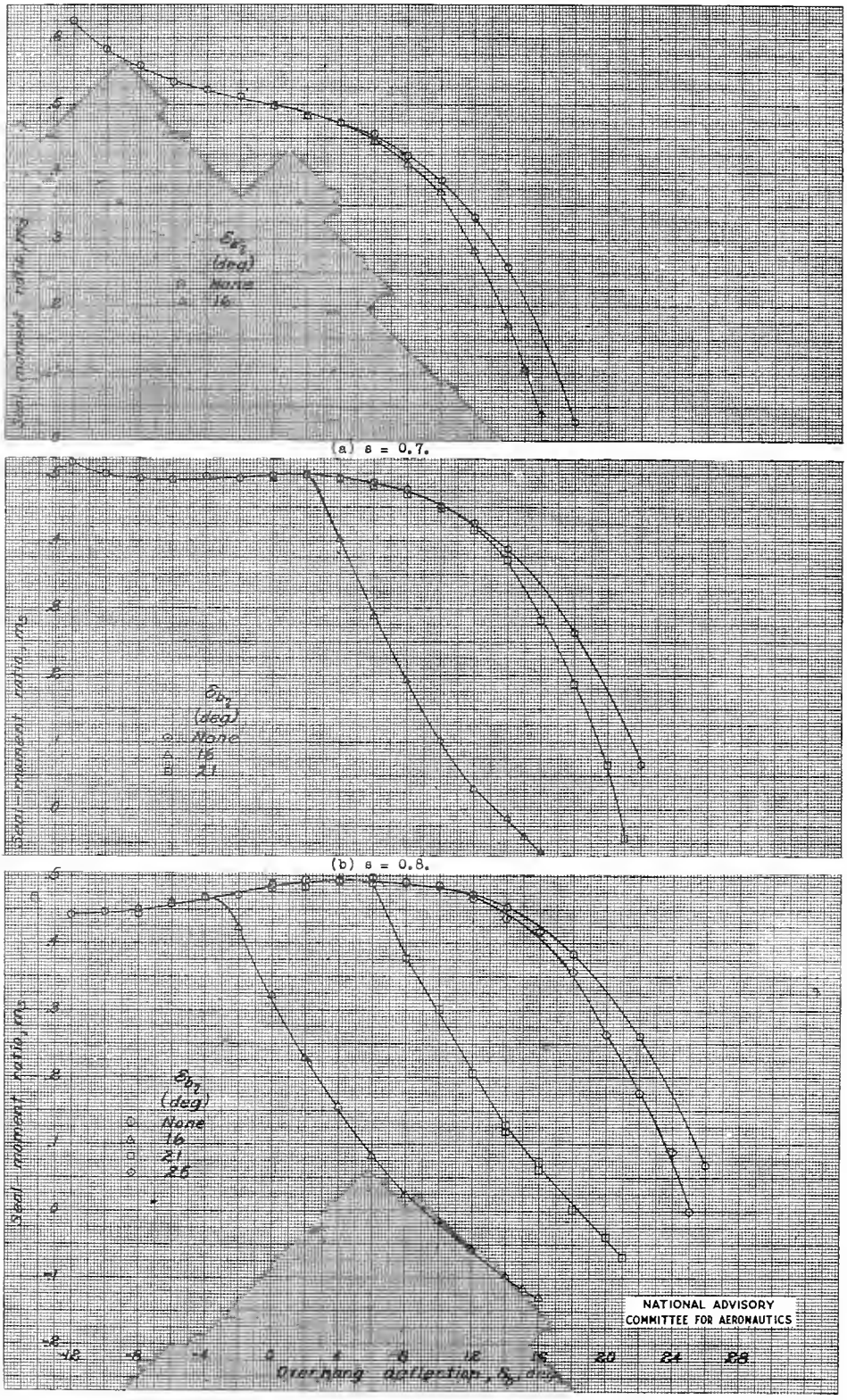

(a) s = 0.7.

(b) s = 0.8.

(c) s = 0.9.

Figure 24.- Hinge-moment characteristics of seals with circular backplate. g = 0.5.

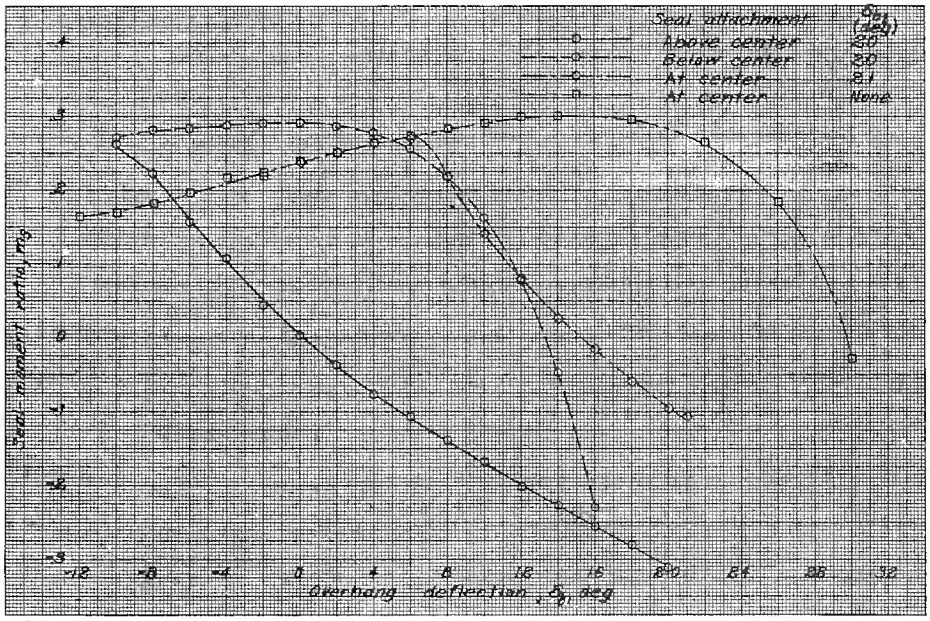

Figure 25.- Hinge-moment characteristics of seals attached $0.34c_b$ off center to circular backplate. $s = 0.8$; $g = 0.3$.

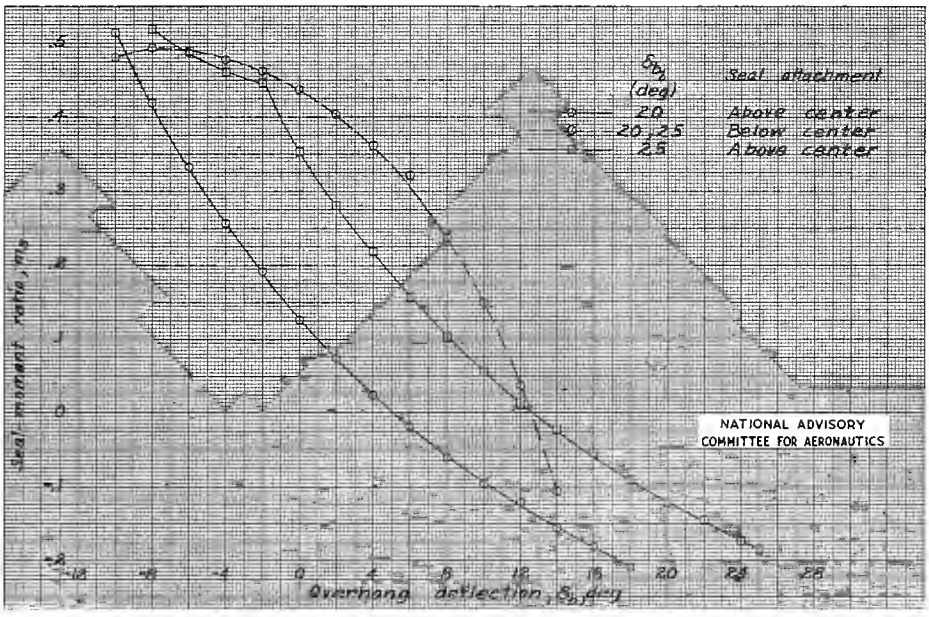

Figure 26.- Hinge-moment characteristics of seals attached $0.34c_b$ off center to circular backplate. $s = 0.9$; $g = 0.5$.

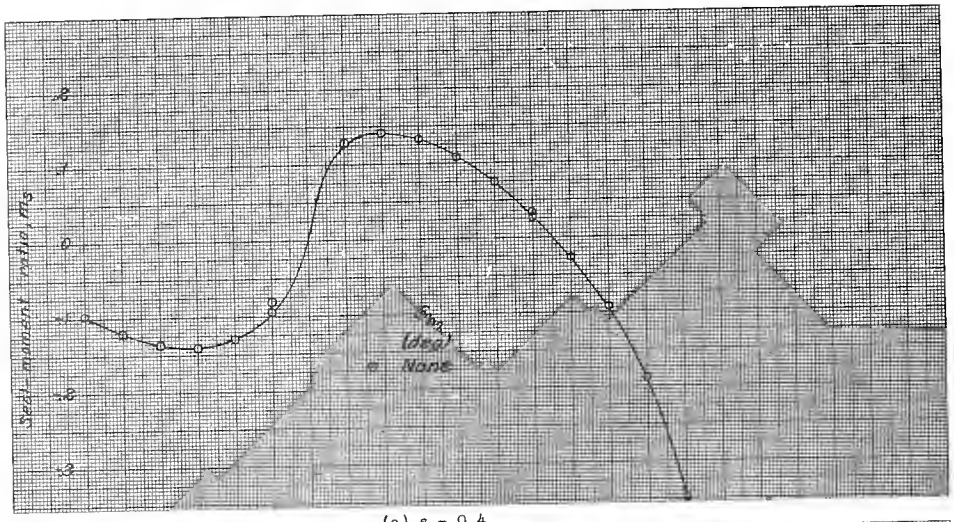

(a) s = 0.4.

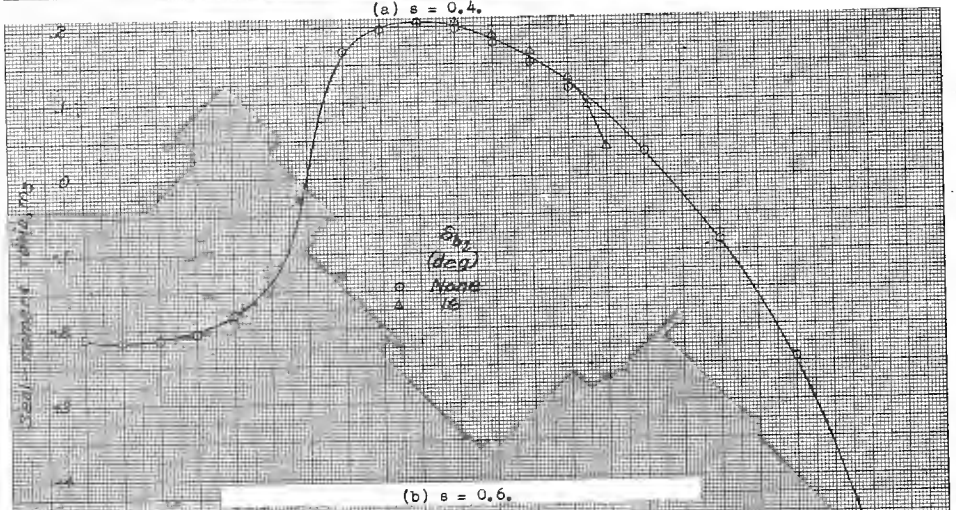

(b) s = 0.6.

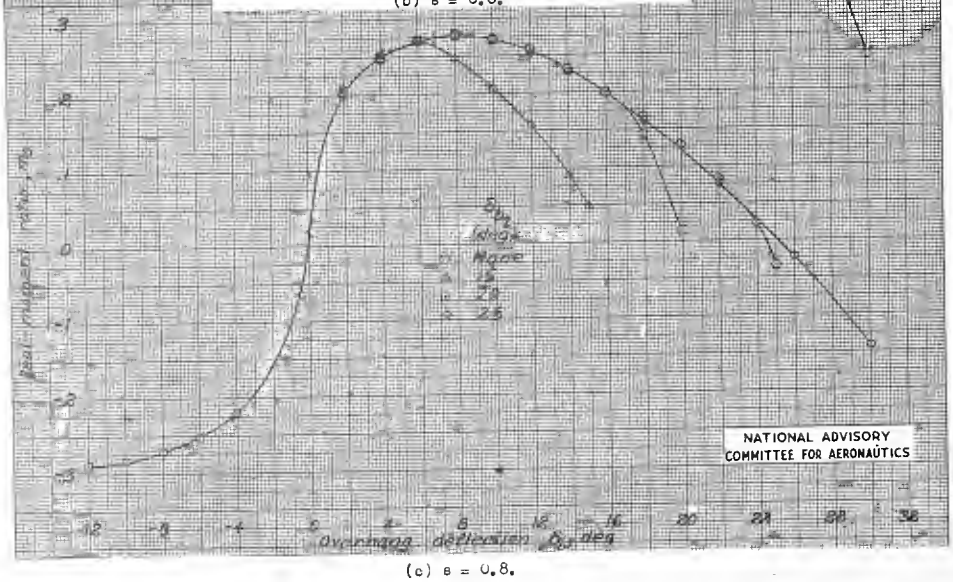

(c) s = 0.8.

Figure 27.- Hinge-moment characteristics of seals with horizontal backplate. g = 0.

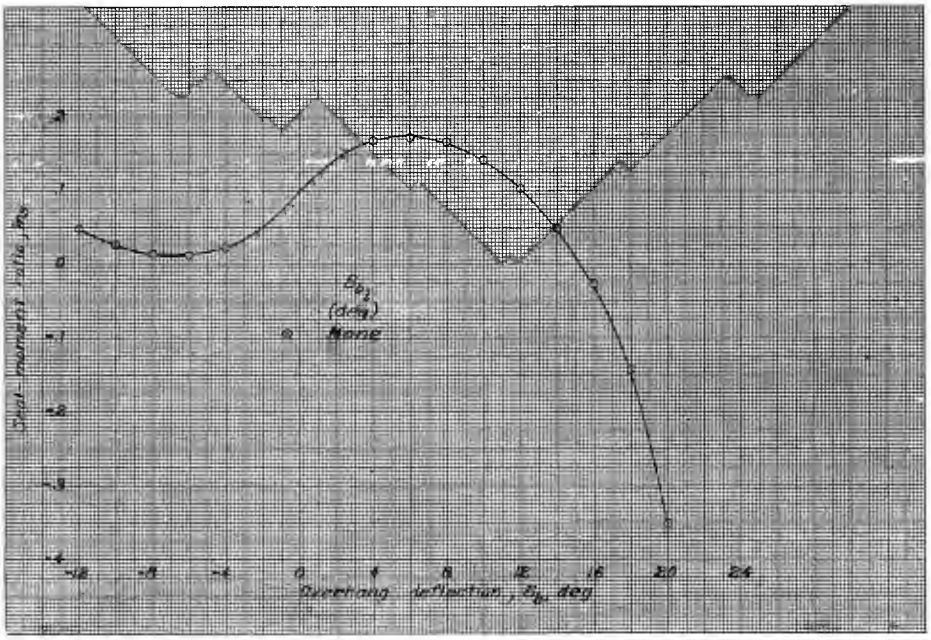

(a) s = 0.4.

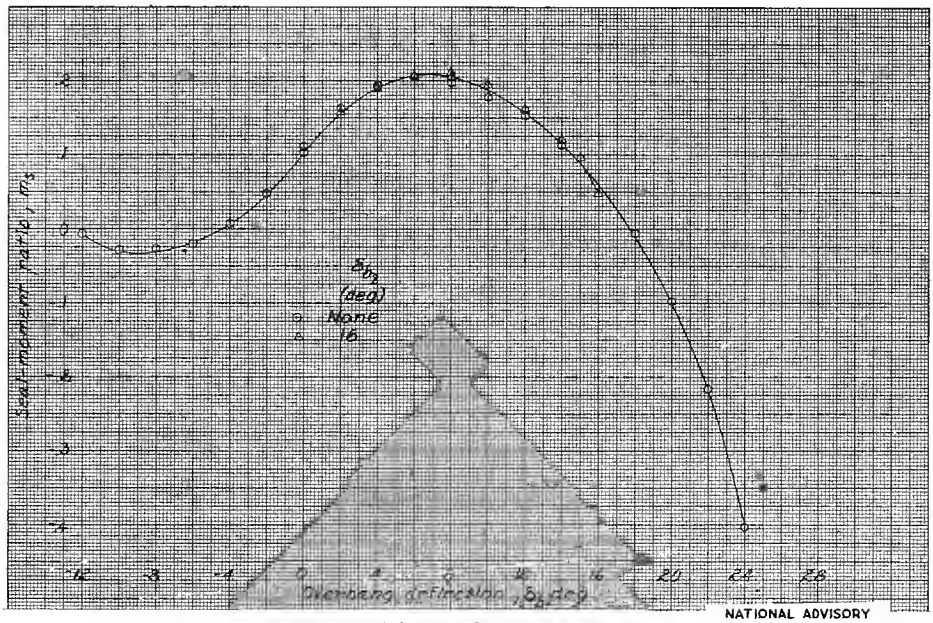

(b) s = 0.5.

NATIONAL ADVISORY COMMITTEE FOR AERONAUTICS

Figure 28.- Hinge-moment characteristics of seals with horizontal backplate. g = 0.1.

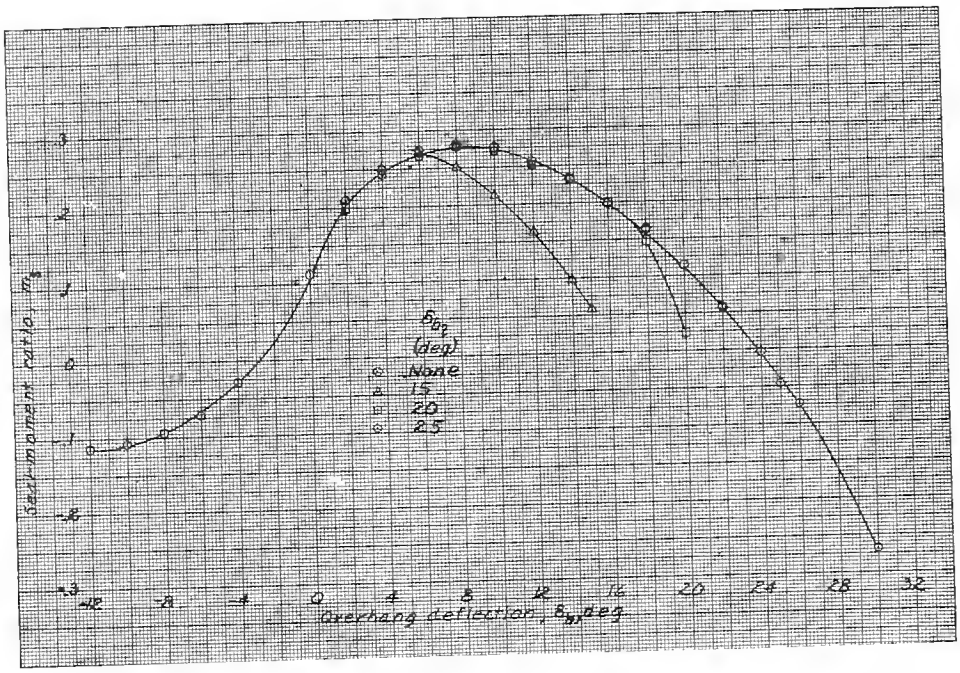

(c) s = 0.7.

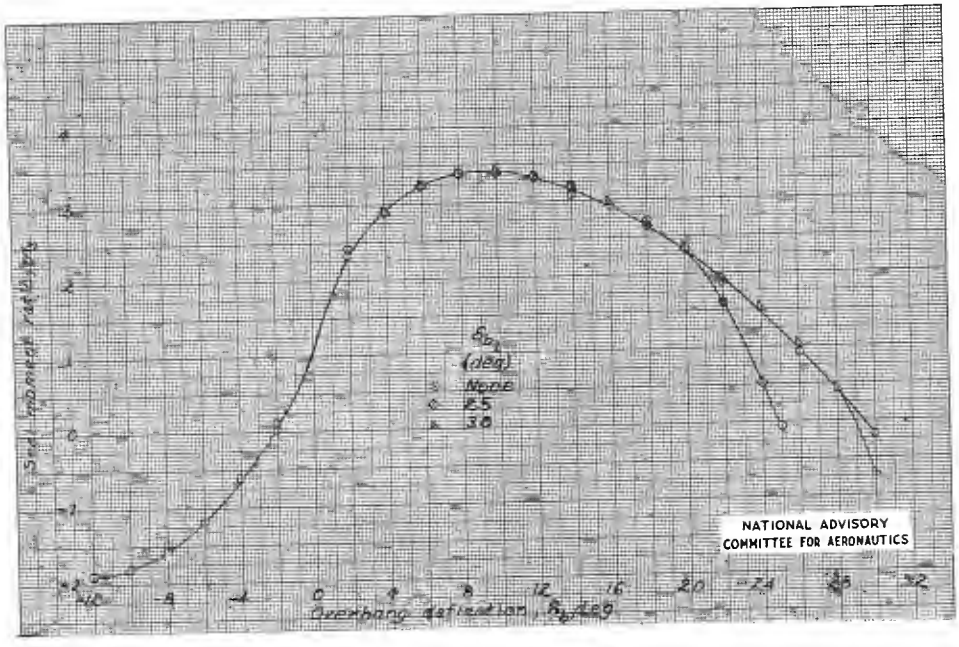

(d) s = 0.9.

Figure 28.- Concluded.

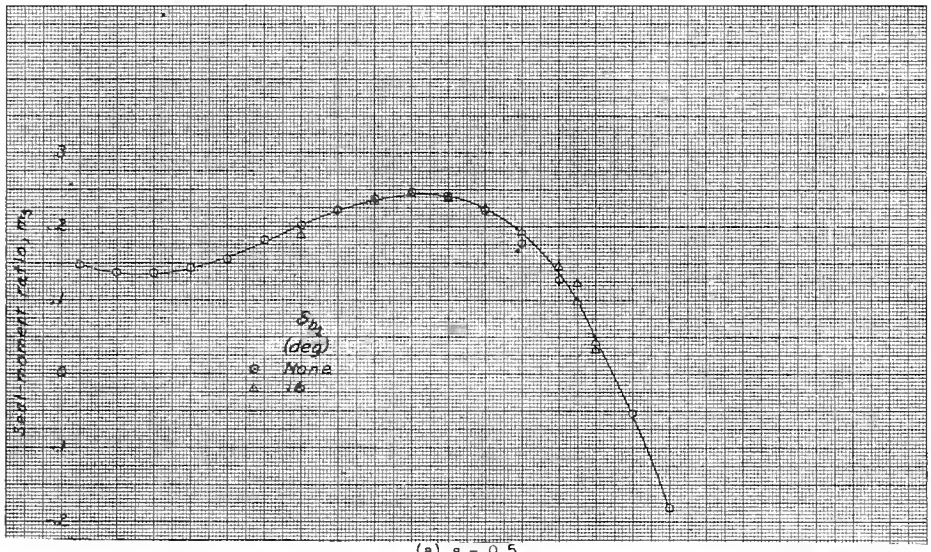

(a) s = 0.5.

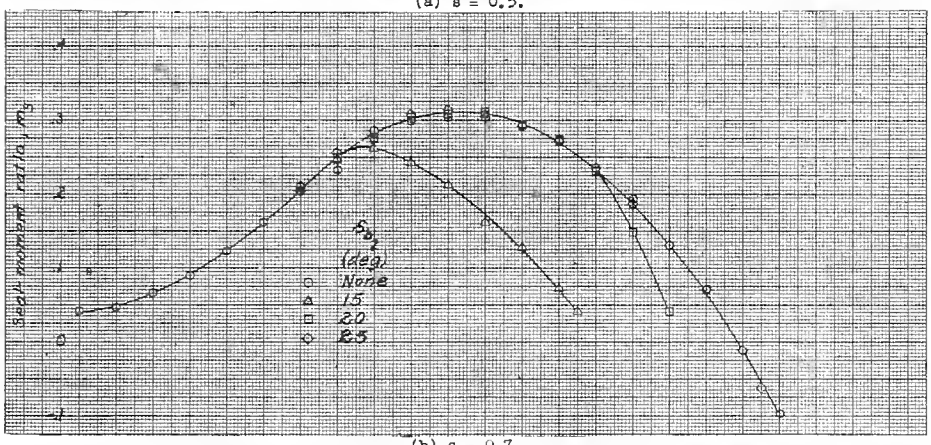

(b) s = 0.7.

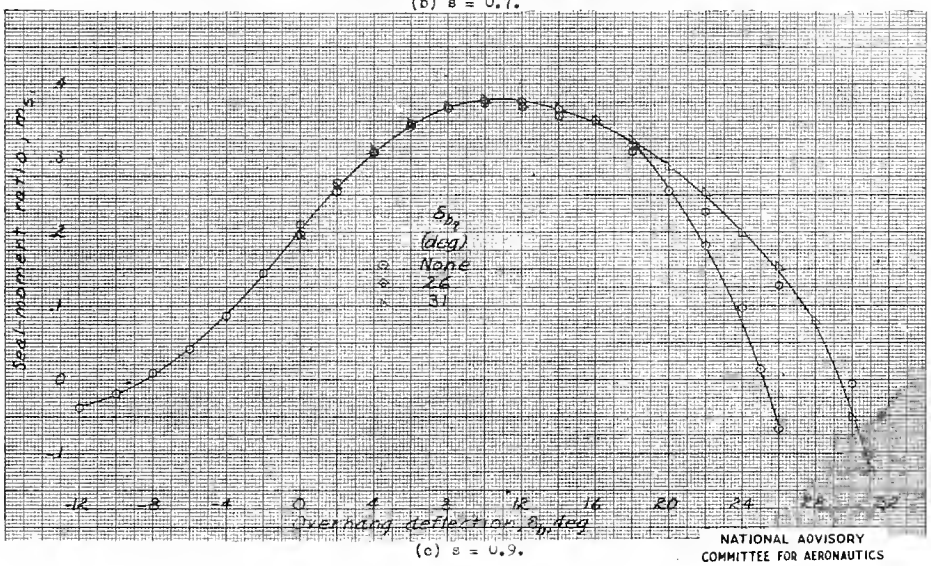

(c) s = 0.9.

Figure 29.- Hinge-moment characteristics of seals with horizontal backplate. g = 0.2.

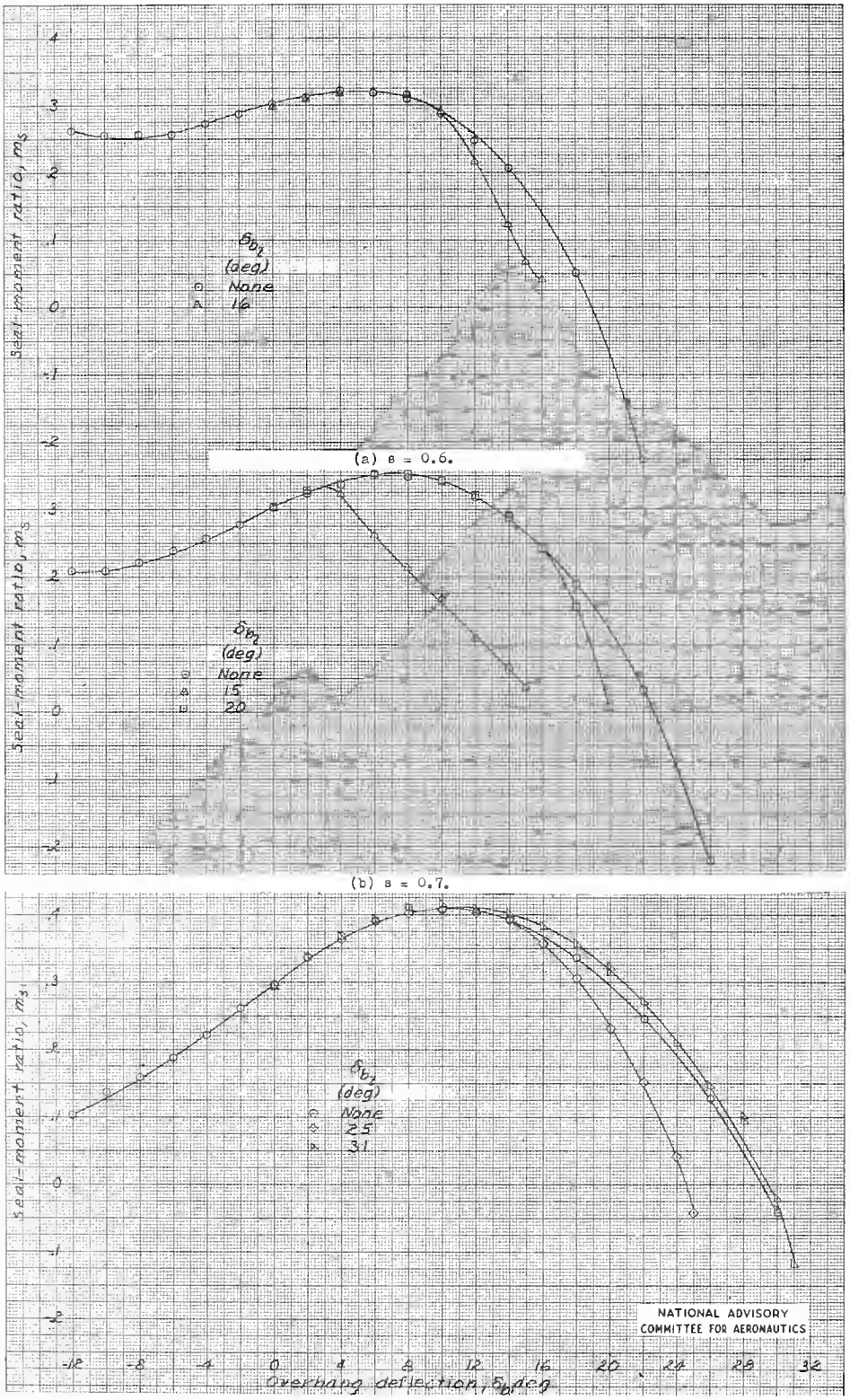

Figure 30.- Hinge-moment characteristics of seals with horizontal backplate. $\bar{c} = 0.3$.

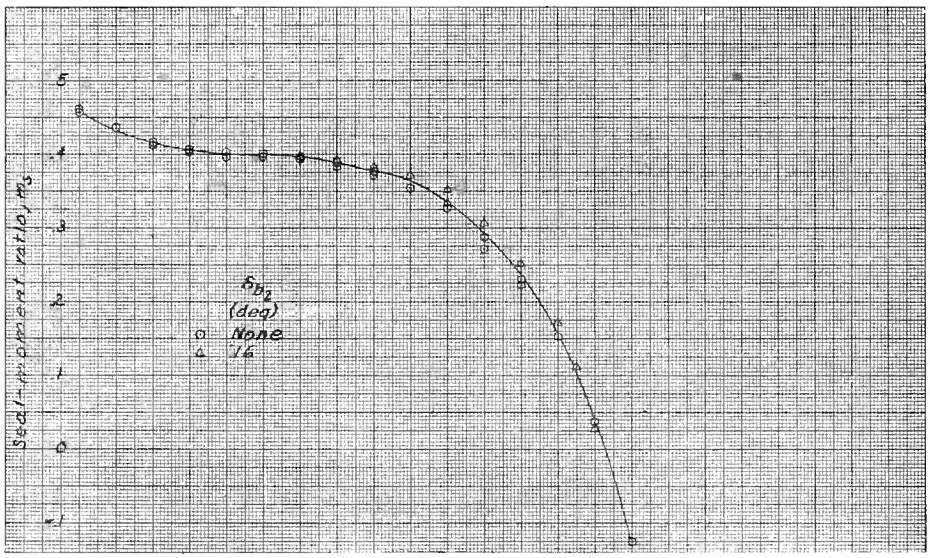

(a) s = 0.6.

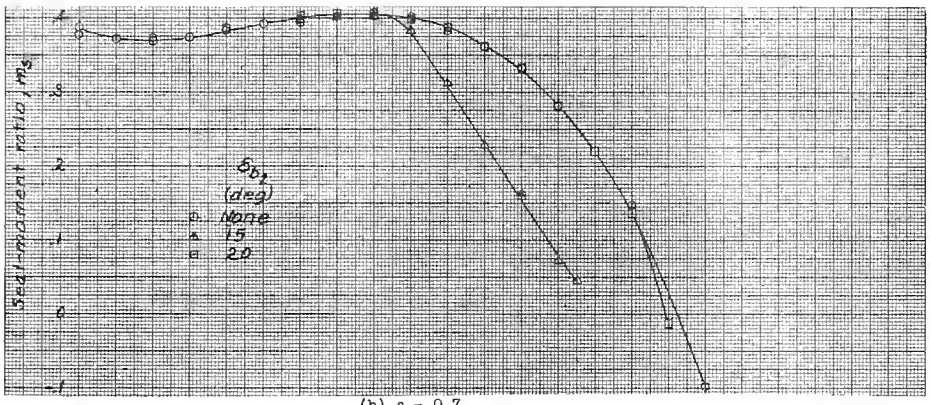

(b) s = 0.7.

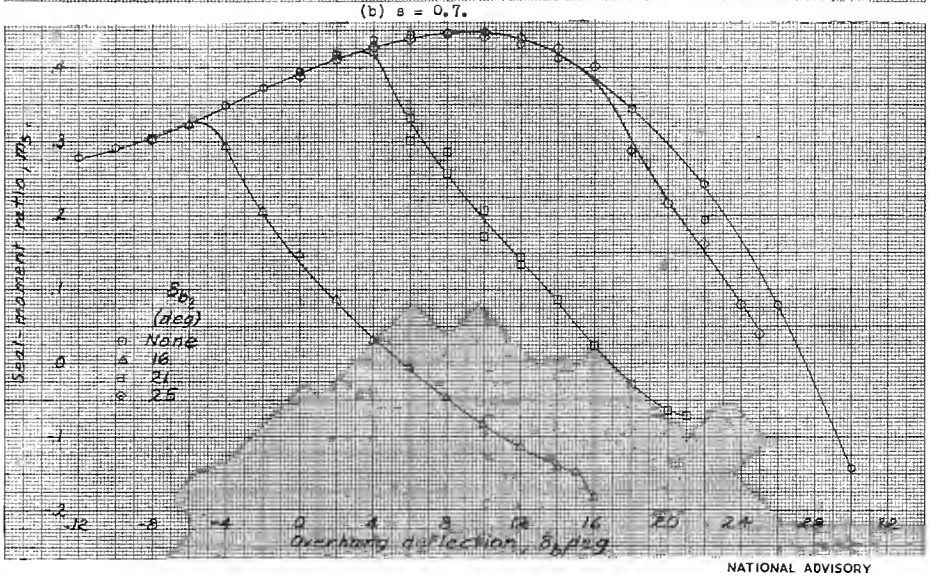

(c) s = 0.9.

NATIONAL ADVISORY COMMITTEE FOR AERONAUTICS

Figure 31.- Hinge-moment characteristics of seals with horizontal backplate. g = 0.4.

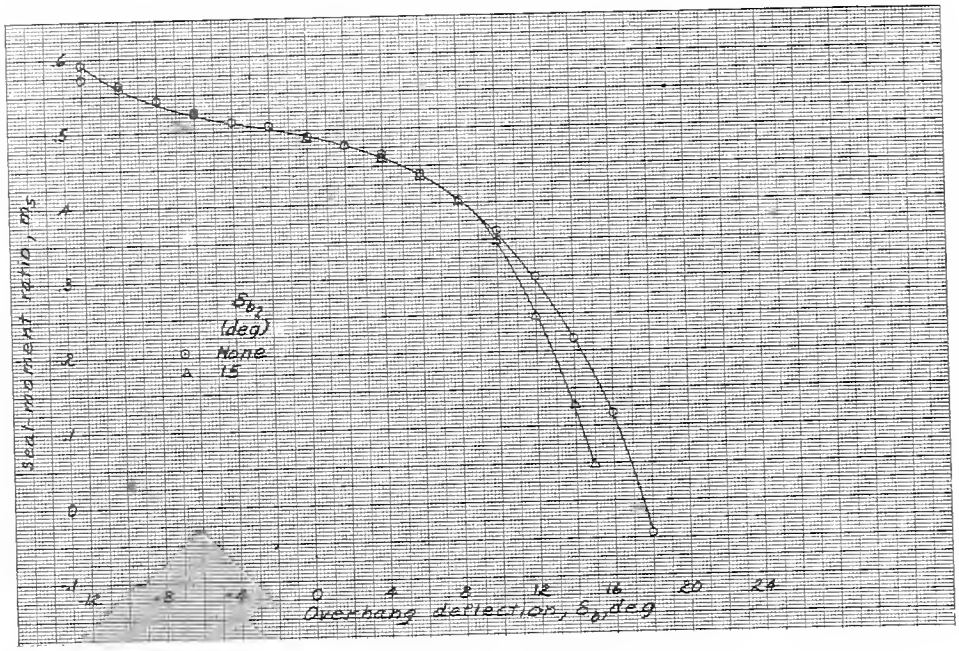

(a) $s = 0.7$.

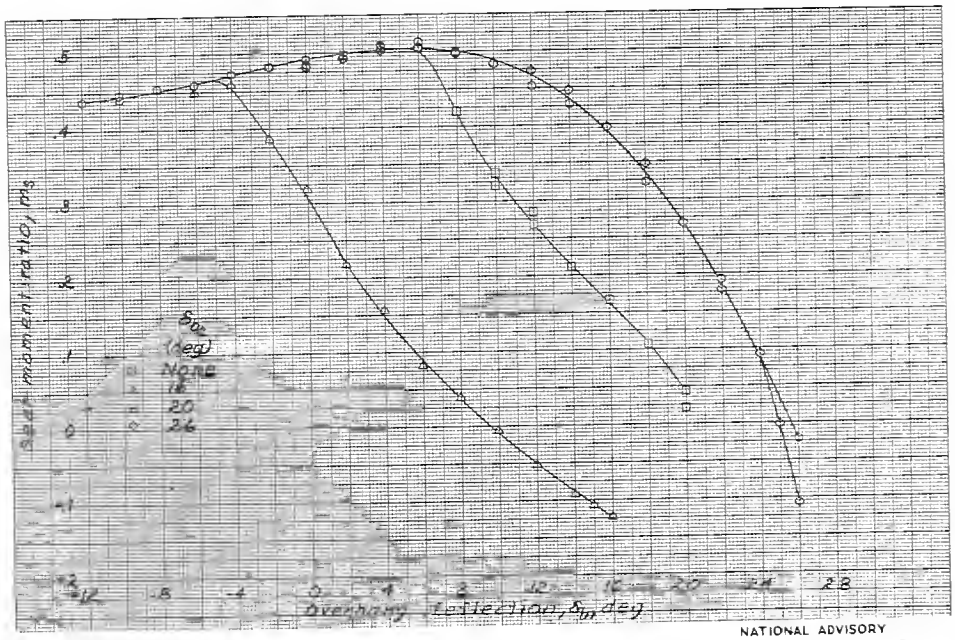

(b) $s = 0.9$

NATIONAL ADVISORY COMMITTEE FOR AERONAUTICS

Figure 32.- Hinge-moment characteristics of seals with horizontal backplate. $g = 0.5$.

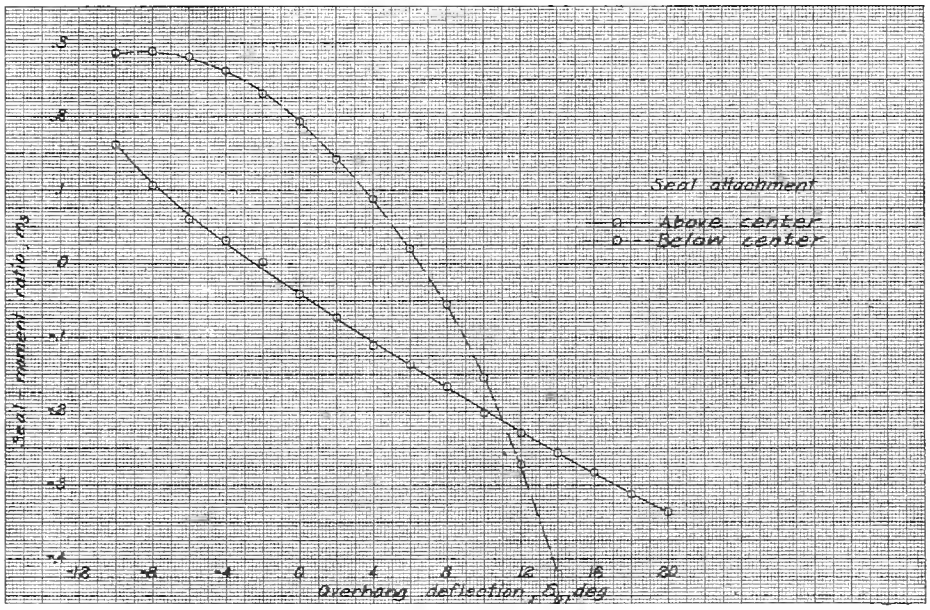

Figure 33.- Hinge-moment characteristics of seals attached $0.34c_b$ off center to horizontal backplate. $e = 0.7$; $g = 0.1$; $\delta_{b_1} = 20°$.

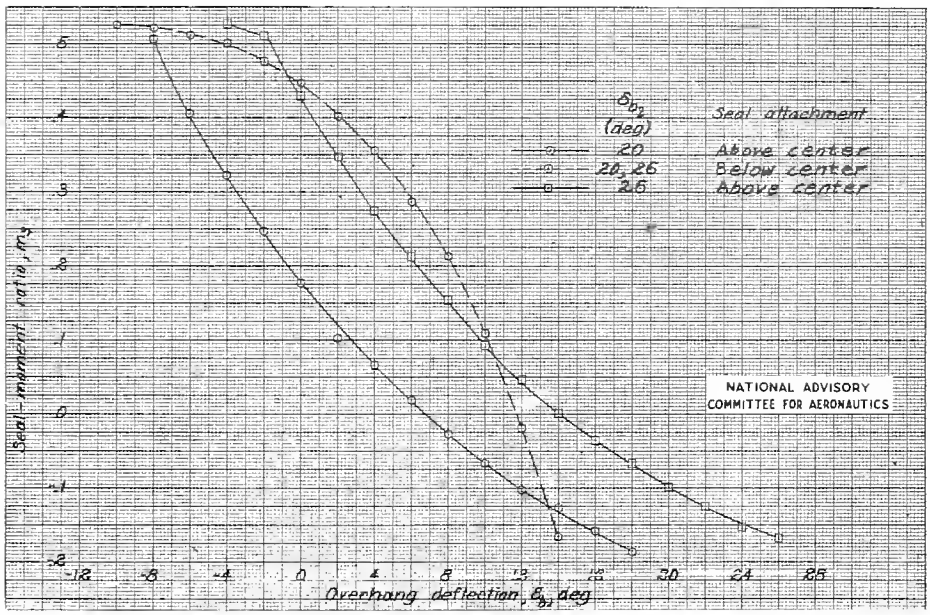

Figure 34.- Hinge-moment characteristics of seals attached $0.34c_b$ off center to horizontal backplate. $s = 0.9$; $g = 0.5$.

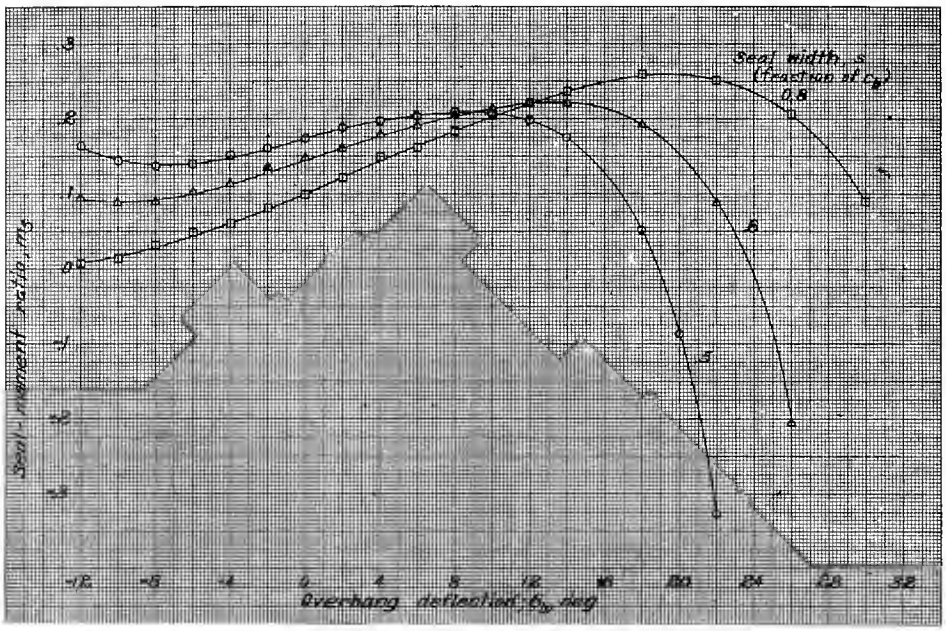

Figure 35.- Effect of seal width on hinge-moment characteristics of seals.
Vertical backplate; g = 0.2; no limiting value for δ_b.

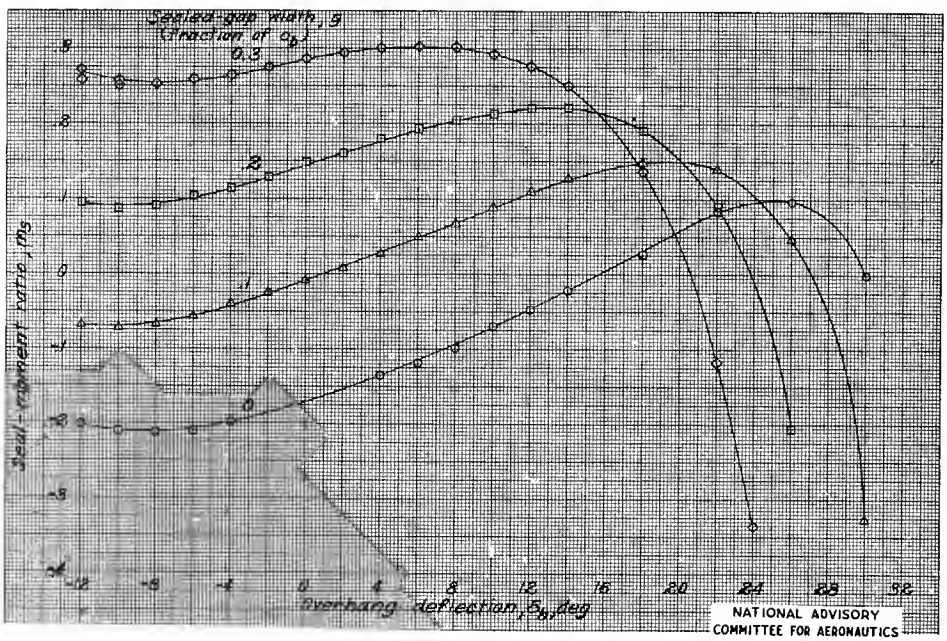

Figure 36.- Effect of sealed-gap width on hinge-moment characteristics of seals.
Vertical backplate; e = 0.6; no limiting value for δ_b.

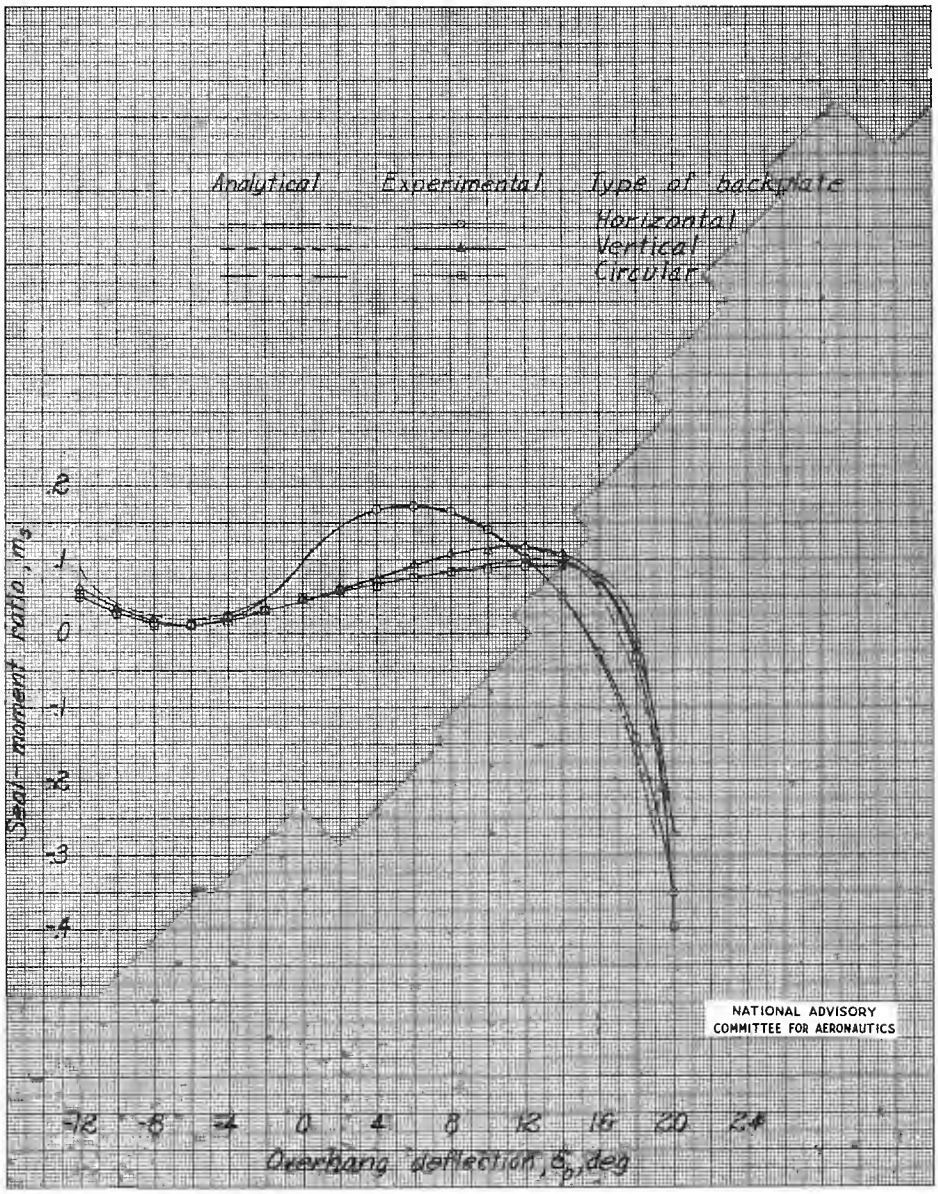

(a) g = 0.1; s = 0.4.

Figure 37.- Comparison of hinge-moment characteristics for seals with vertical, horizontal, and circular backplates.

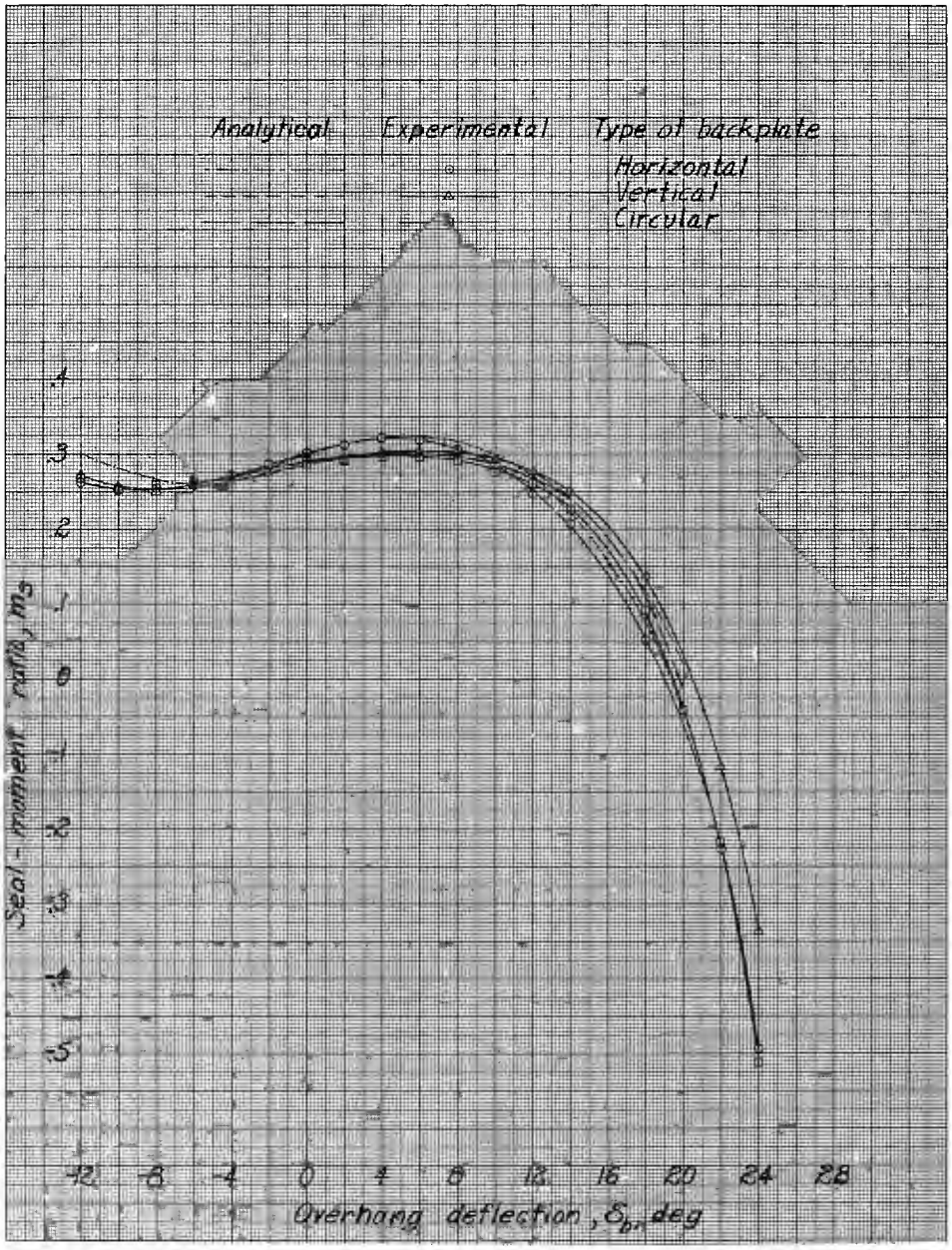

(b) g = 0.3; s = 0.6.

Figure 37.- Continued.

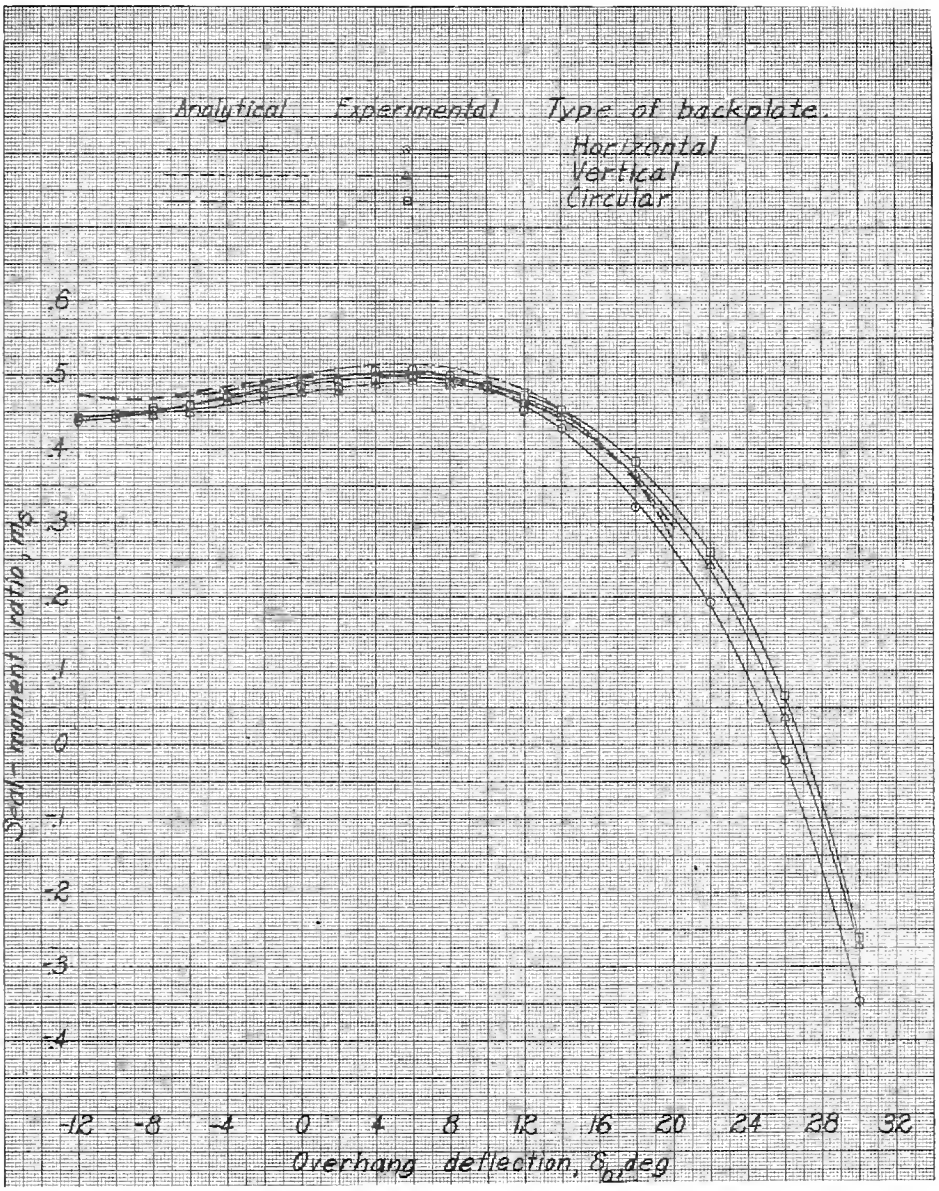

NATIONAL ADVISORY
COMMITTEE FOR AERONAUTICS

(c) g = 0.5; s = 0.9.

Figure 37.- Concluded.

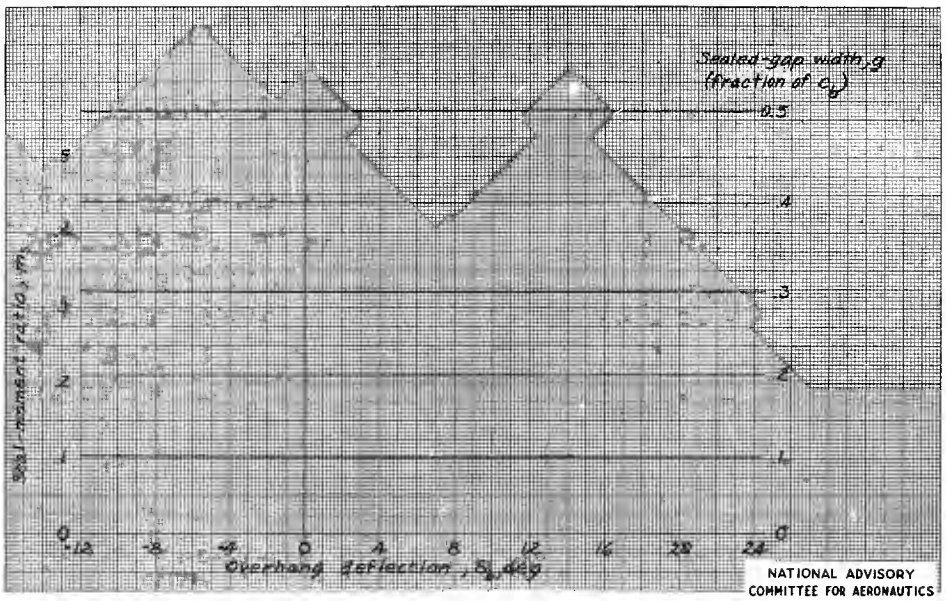

Figure 38.- Seal-moment ratio computed by approximate method (measuring balance chord to center of gap) for various sizes of sealed-gap width.

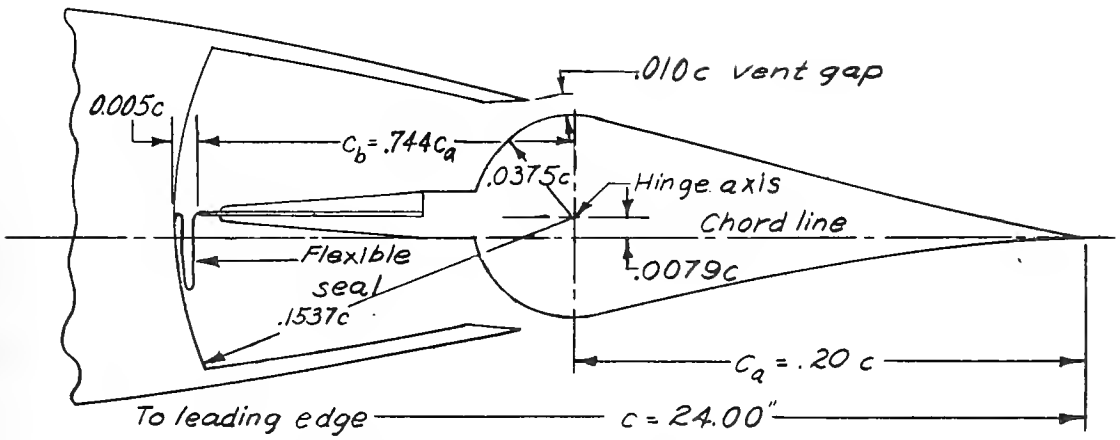

(a) Sealed internally balanced aileron.

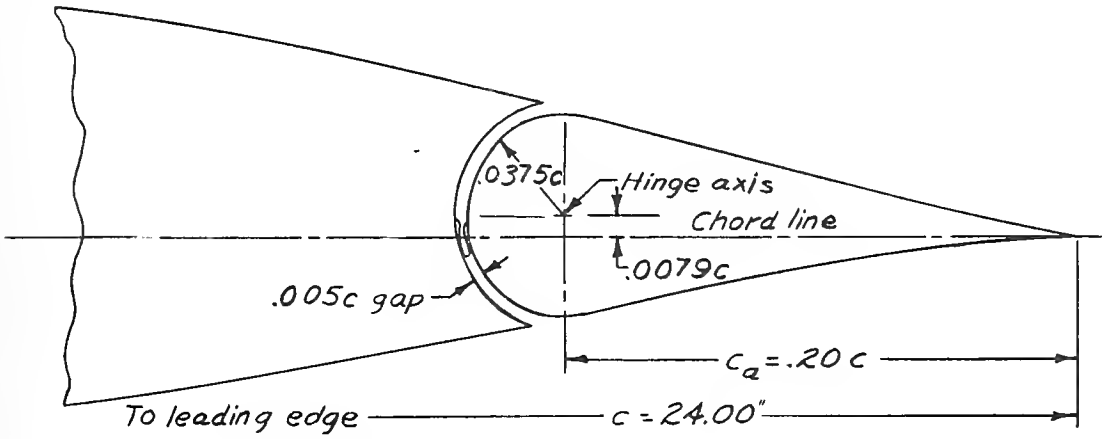

(b) Plain sealed aileron.

NATIONAL ADVISORY COMMITTEE FOR AERONAUTICS

Figure 39.- True-contour aileron sections for which illustrative data are presented.

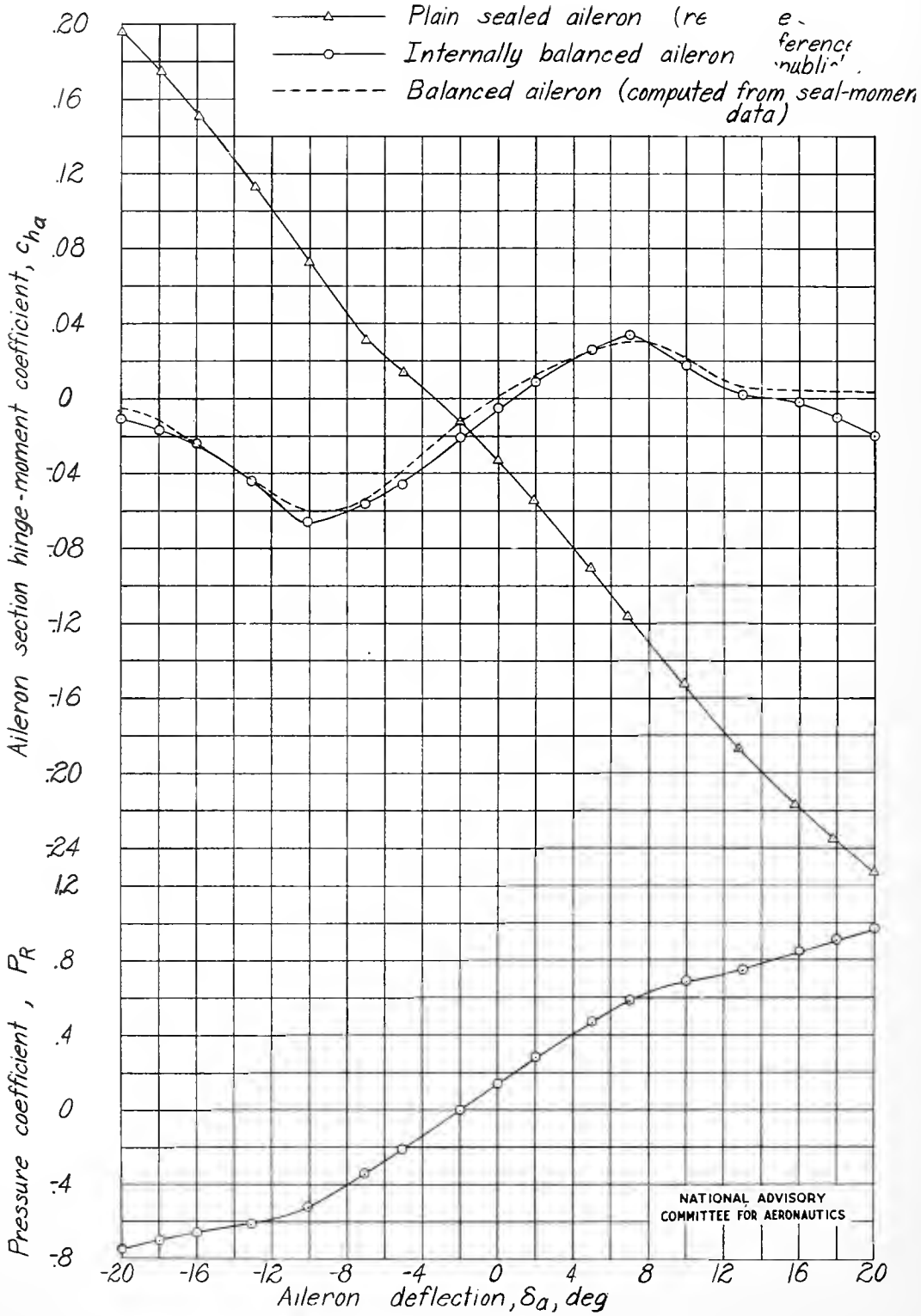

Figure 40.- Comparison of section hinge-moment characteristics measured on sealed internally balanced aileron with characteristics computed from plain sealed aileron. True-contour ailerons of 0.20c on an airfoil. $\alpha = 0^{\circ}$; $M = 0.36$.

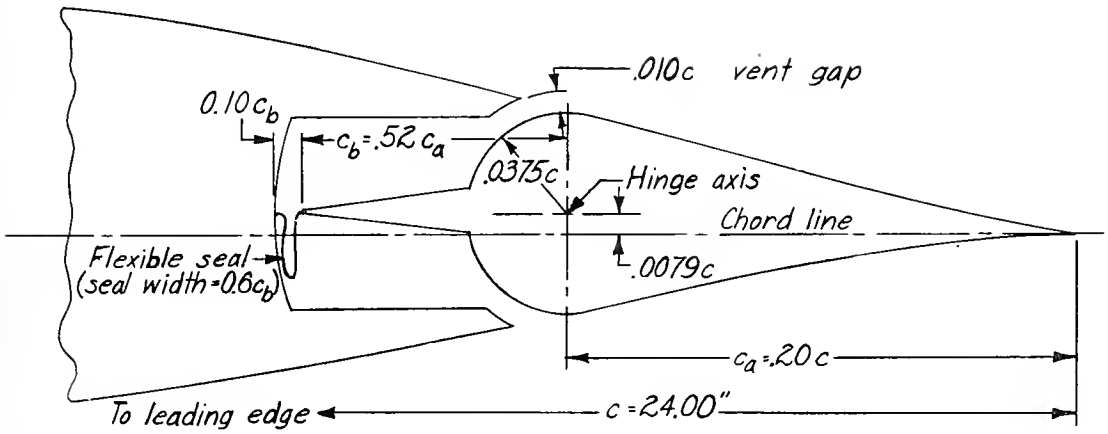

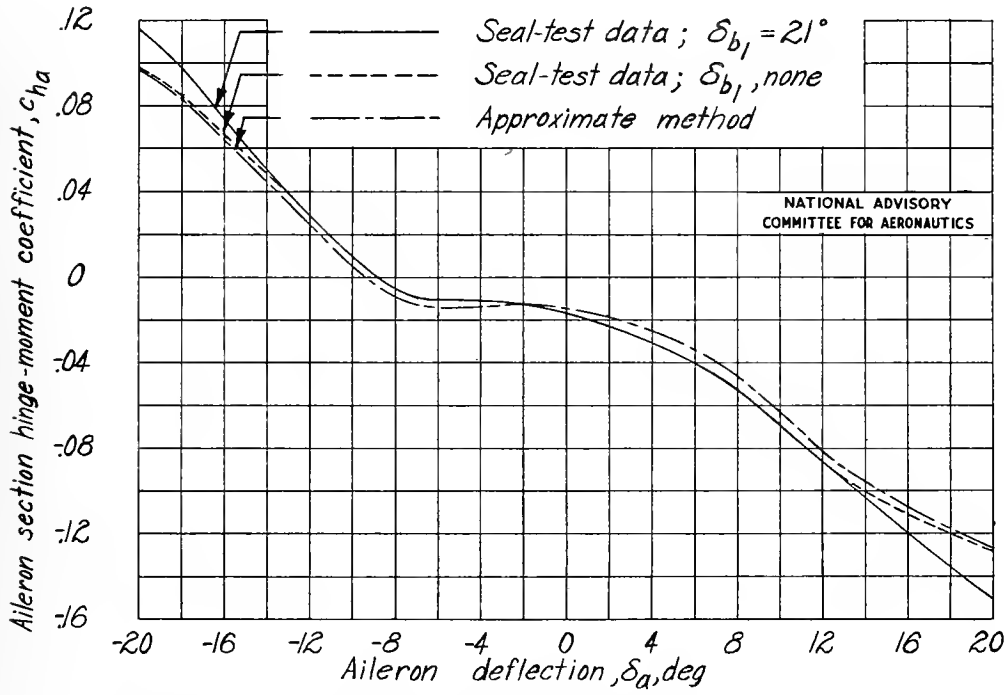

Figure 41.- Comparison of section hinge-moment characteristics of sealed internally balanced aileron computed from seal-moment data and by approximate method. True-contour aileron of 0.20c on an airfoil. $\alpha = 0^{\circ}$; M = 0.36. (Pressure data and plain-aileron hinge-moment data from fig. 40.)